

The **RISING** Project

Proposals for Fast Beam Configuration



RISING Collaboration

June 2002

In-beam γ -Spectroscopy at Relativistic Beam Energies with RISING at the FRS

*P. Reiter (Univ. Köln) for the RISING Collaboration**

1. Introduction

The SIS/FRS facility provides secondary beams of unstable rare isotopes after fragmentation reactions or secondary fission of relativistic heavy ions with sufficient intensity for in-beam γ -spectroscopy measurements. The proposed experiments for the first RISING (Rare ISotope INvestigations at GSI) campaign will exploit these unique beams at relativistic energies in the range from 100 MeV/u to 400 MeV/u. Most of the experiments depend on fragmentation products from heavy primary beams and are only feasible at GSI. The RISING spectrometer will be employed not only for relativistic Coulomb excitation but also for pioneering high-resolution γ -spectroscopy experiments after secondary nucleon removal reactions and secondary fragmentation. New experimental methods for spectroscopy at relativistic energies will be investigated in order to obtain important nuclear structure observables beyond the directly accessible level energies and quadrupole deformations. Several proposals focus on new methods and techniques in order to determine magnetic moments and life times of short lived states, properties of isomeric states and spectroscopic factors at relativistic energies for the first time.

The motivations to explore nuclear structure of exotic nuclei focus on the following subjects:

- Shell structure of instable doubly magic nuclei and their vicinity.
- Symmetries along the N=Z line and mixed symmetry states.
- Shapes and shape coexistence.
- Collective modes and E1 strength distribution.

Shell structure

Spectroscopic data on the single particle structure of instable doubly magic nuclei and their nearest neighbours are pivotal for theoretical description of the effective interactions in large-scale shell-model calculations. The proposed studies around the N=Z doubly magic nuclei ^{56}Ni and ^{100}Sn provide an excellent probe for single-particle shell structure, proton-neutron interaction and the role of correlations, normally not treated in mean field approaches. The $B(E2, 2^+ \rightarrow 0^+)$ values in semi-magic Sn nuclei provide a sensitive test for changing (sub)shell structure, the E2 polarisability and the shape response of the magic core. For several reasons conventional techniques, employing (HI,xn) reactions, are very difficult or even impossible and the proposed Coulomb excitation measurements are the only way to obtain the information needed to investigate the evolution of shell structure close to the proton drip line.

Beyond the very neutron-rich shell closures from ^{34}Si to ^{132}Sn the possible disappearance of the familiar Woods-Saxon shell closures and their reappearance as harmonic magic numbers is predicted by several mean-field calculations. Moreover, ^{78}Ni and ^{132}Sn are located close to the astrophysical rapid neutron capture process path and indirect evidence for an altered shell structure and shell quenching of magic gaps at N=82 and N=126 is derived from recent r-process network calculations. Alternatively, observed new shell structure in light and medium-heavy nuclei can be qualitatively understood in terms of monopole shifts of selected nucleon orbitals, with deviating predictions for new shell gaps and spin-orbit splitting. To date the investigative methods have not been able to gather information in the region of neutron-rich Ni and Sn isotopes about the most significant matrix elements, the magnetic moments and the spectroscopic factors, which are sensitive indicators of their structure.

Symmetries

The validity of the isospin symmetry for the strong interactions is a fundamental assumption in nuclear physics and the degree to which this symmetry holds as the proton drip line is approached, remains an open question. Experimentally, the symmetry shows as nearly identical spectra in pairs of mirror

* see Annex B1

nuclei obtained by interchanging protons and neutrons. A slight breakdown of the symmetry arises from the Coulomb interaction, causing small differences in excitation energies between isobaric analog states. The Coulomb energy differences between excited analog states in mirror nuclei have been studied for proton rich ($N=Z-2$) isobars in the $A=50$ region revealing subtle nuclear structure effects as a function of spin and energy. RISING will facilitate experimental studies of medium mass mirror nuclei with larger values of isospin $T \geq 3/2$ in order to provide rigorous tests of large-scale pf-shell model calculations.

Within the framework of the proton-neutron version of the interacting boson model (IBM-2) the existence of low-lying valence shell excitations, which are not symmetric with respect to the proton-neutron degree of freedom, are predicted. These states are called mixed-symmetry states and are e.g. established in all stable $N=52$ isotones. Coulomb excitation experiments with radioactive beams are required to observe the evolution of these states for lighter $N=52$ isotones below $Z=40$.

Collective Excitations

Collective excitations such as the giant dipole resonance (GDR), built from collections of single-particle excitations are necessarily influenced by the nuclear shell structure. In exotic nuclei like $^{68-78}\text{Ni}$ the proton-neutron asymmetry may give rise to differing shell structure. Theoretical calculations predict a significant change in the GDR strength distribution as one progresses towards the doubly magic ^{78}Ni . The excitation function of the isovector GDR mode is expected to fragment substantially, favoring a redistribution of the strength towards lower excitation energies (Pygmy resonance). Measurements of the GDR strength function provide access to the isospin dependent part of the in-medium nucleon-nucleon interaction and on dipole type vibrations of the excess neutrons. The predicted low-energy shift of the GDR strength was confirmed in neutron-rich oxygen isotopes by the LAND group at GSI by means of virtual photon absorption measurements. The proposed GDR experiment in ^{68}Ni will apply a complementary method, virtual photon scattering, which relies on real projectile γ -ray emission following the virtual excitation. In order to observe discrete γ -transitions with high resolution and γ -decay from the GDR, the RISING array will be augmented by BaF scintillators.

Shapes

The phenomenon of shape coexistence is caused by various structure effects, which can be traced back to the polarisation by high spin intruder orbitals, which happens to occur primarily in exotic regions of the Segré chart. Along semi magic isotopic and isotonic chains midshell between shell closures 2p-2h and 4p-4h excitations across the shell gap into high-spin orbitals cause coexistence of spherical, oblate and prolate shape as seen in the Pb ($Z=82$) isotopes, so far without firm experimental assignment of the specific shape. Aided by shell gap melting, even the ground state may become deformed as in the well known $N=20$ nucleus ^{32}Mg . High-K isomers, built by multi-quasi particle configurations, due to their influence on the amount of pairing and/or collectivity left, may give rise to shape changes. Most often deformed nuclei obey axial and reflection symmetry. However, in specific nuclear regions where the Fermi level approaches pairs of close lying, opposite-parity orbitals with $\Delta j = \Delta l = 3$ reflection asymmetric shapes are predicted, e.g. the heavy Ba nuclei may show octupole deformed states.

2. Experimental Technique

All individual experiments described in this proposal will use the same general technique introduced below. A basic set-up also described here will be employed in most cases. Therefore, the individual proposals concentrate on their specific physics case and rate estimate, while experimental details are only given for non-standard parts of the set-up.

The proposed γ -ray spectroscopy of nuclei from exotic beams will be performed after in-flight isotope separation. The exotic beams will be produced by fragmentation of a heavy stable primary beam or fission of a ^{238}U beam on a ^9Be or ^{208}Pb target (typical thickness $\approx 1\text{g/cm}^2$) in front of the fragment separator, FRS. A maximal beam intensity from the SIS synchrotron of $10^{10}/\text{s}$ for medium heavy beams (e.g. ^{129}Xe) and $10^9/\text{s}$ ^{238}U is expected. The secondary beam intensities entering the rate estimates are easily calculated from

$$\text{fragments [s}^{-1}] = \text{target nuclei [cm}^{-2}] \cdot \text{beam intensity [s}^{-1}] \cdot \text{cross section [cm}^2],$$

with cross sections for fragmentation reactions taken from the EPAX parameterisation, and from listed experimental data for fission processes.

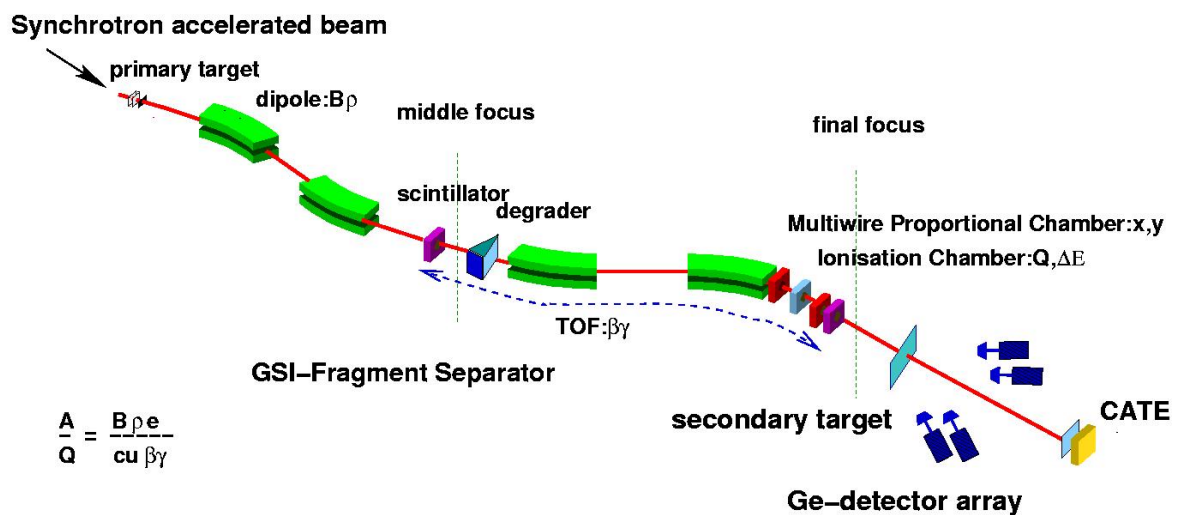


Fig. 1: *The RISING fast beam set-up at the FRS.*

Particle identification and tracking

The FRS will be operated in a standard achromatic mode, which allows a separation of the species of interest by combining magnetic analysis with energy loss in matter. The transmission through the FRS is typically 20-30% for fragmentation and 1-2% for fission (depending on the actual isotope). The separated ions will be identified on an event-by-event basis with respect to mass and atomic number via combined time-of-flight, position tracking, and energy loss measurement. As shown in figure 1 this is achieved with plastic detectors, MWPC's and a MUSIC chamber optimised for high event rates ($\leq 50\text{ kHz}$).

After passing the identification set-up, the radioactive ions at relativistic energies are focussed onto a secondary target, positioned approximately 4m behind the last FRS magnet in the experimental area S4. Massive slits, absorbing most of the radiation produced by hitting ions, are foreseen to reduce the amount of unwanted species reaching the secondary target. Behind the target the calorimeter telescope, CATE, will be used for channel selection. CATE consists of position sensitive Si ΔE detectors (lab.

angular range $\pm 3^\circ$) with a charge resolution of $\approx 1/100$ and CsI scintillators for total energy measurement with a measured resolution of $\approx 1/100$. It is assumed that the kinetic energy loss of a projectile-like nucleus due to nuclear excitation is negligible and thus the velocity behind the secondary target does not differ significantly from the velocity of those projectiles, which do not undergo nuclear interaction. In that case the mass of the projectile-like nucleus can be taken from the total energy without additional time-of-flight measurement. For heavy nuclei the mass resolution is not sufficient to discriminate single masses. However, due to the high resolution of the γ detectors and the expected low to medium γ multiplicities this is generally not required. The identification of a nucleus by gating on its characteristic γ line is of course always possible.

Gamma detection

For the excited fragments moving at a high velocity ($v/c = 0.43$ at a fragment energy of 100 MeV/u) the γ detectors have to be positioned at either forward or backward angles in order to minimize Doppler broadening. The distance to the target depends on the required energy resolution. The best possible configuration of the 15 Cluster detectors available for experiments with fast beams is displayed in figure 2.

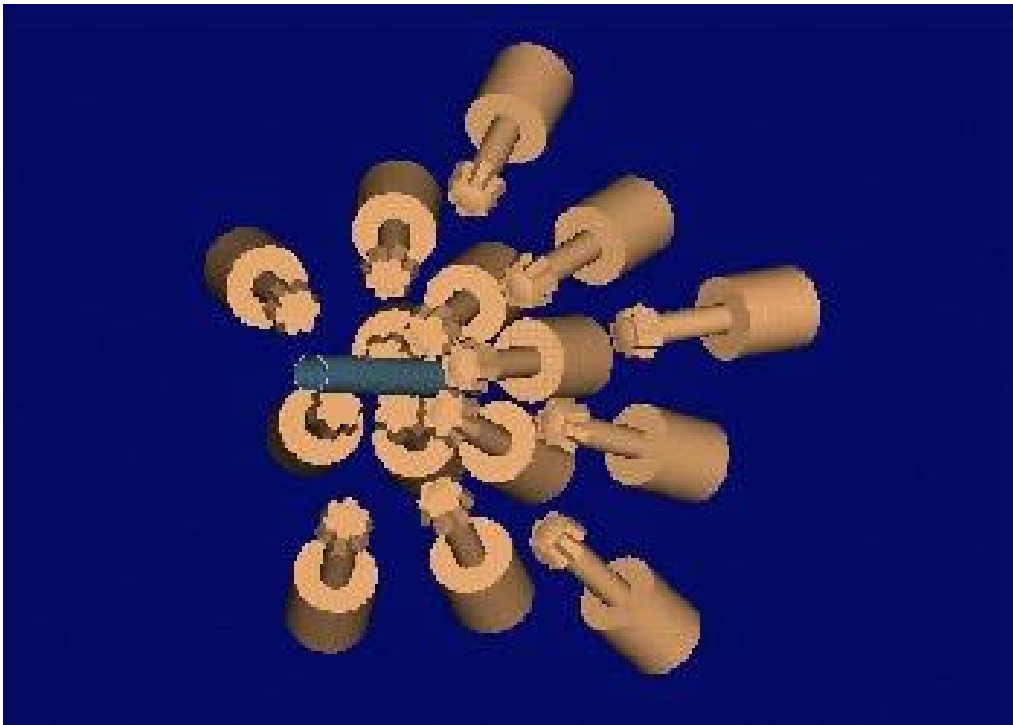


Fig. 2: Configuration of 15 Cluster Ge-detectors without BGO shields for experiments with relativistic beams.

Due to the Lorentz boost the main efficiency contribution comes from the first ring. This ring is positioned to achieve 1% resolution within the constraints of the beam pipe diameter of 16cm. One should note that the 5 Clusters in the 2nd and 3rd rings could be moved closer to the target position, for an increased efficiency but a lower overall resolution. Table 1 summarizes the positions of the detectors. If a γ -ray energy resolution of 1% is required the target distance of ring two (three) needs to be 112 cm (137 cm). In that case the total full energy efficiency at 1.3 MeV is 1.7% for γ rays emitted in flight ($v/c=0.43$).

If both rings are placed at a minimum distance of ~70cm then the configuration will reach a total efficiency of 2.9% while the average weighted energy resolution is only slightly increased to 1.24%.

Table 1: Position and distances of the Cluster detectors.

| | Cluster detectors | Angle | Target distance |
|---------|-------------------|-------|-----------------|
| Ring #1 | 5 | 15.0° | 680 mm |
| Ring #2 | 5 | 26.5° | 680 - 1400 mm |
| Ring #3 | 5 | 34.0° | 680 – 1400 mm |

3. Proposed experiments

Within this campaign 12 experiments are being proposed as shown in table 2. No. 1 is only included for completeness since it has already been accepted in 1999 by the GSI Experimentausschuss as part of the γ -spectroscopy program with the Vega set-up but is suggested to be performed with the RISING set-up. The specific physics case and rate estimates for all experiments are described in the annex. The primary beams and the requested running time is shown in Table 2. The total of **86 days** does not include the FRS preparation time, which can be reduced to **7 days** of main beam time by running in suitable blocks. For commissioning of RISING experiment No. 8 is foreseen. Additional commissioning and preparation of the individual set-ups will be done parasitic.

Table 2: Summary of the experiments proposed for the fast RISING campaign.

| No. | Nuclei of Interest | Primary Beam | Spokespersons | Experiment Type | Request (days) |
|----------|--|-------------------------------------|-------------------------------------|---------------------------------------|----------------|
| 1 (S244) | ^{34/36} Mg | ⁴⁸ Ca | P. Mayet | 2 step fragmentation lifetime | 6 (Accepted) |
| 2 | ⁴⁵ Cr, ⁵³ Ni, ⁴⁵ Sc, ⁵³ Mn | ⁵⁸ Ni | M. Bentley | 2 step fragmentation | 7 |
| 3 | ⁶⁸ Ni | ⁸⁶ Kr | A. Bracco | GDR | 7 |
| 4 | ⁵⁴ Ca, ⁷⁸ Ni | | H. Grawe, H. Hübel, P.Reiter | Coulex | 13 |
| 5 | ⁸⁸ Kr, ⁹⁰ Sr, ⁸⁶ Se | ²³⁸ U | D. Tonev | Coulex | 10 |
| 6 | ¹⁰²⁻¹¹⁰ Sn, ⁹⁴⁻⁹⁸ Ru | ¹²⁴ Xe | C. Fahlander, M. Górska | Coulex | 6 |
| 7 | ¹³² Sn | ²³⁸ U | G. de Angelis | Knock-out | 5 |
| 8 | ¹³² Xe | ¹³⁶ Xe | A. Maj | Coulex, Angular Distr. / Correlations | 3 |
| 9 | ¹³⁴ Te | ¹³⁶ Xe | K.-H. Speidel | Coulex, g-factor | 7 |
| 10 | ¹⁴²⁻¹⁴⁶ Ba | ¹⁵⁰ Nd | S. Mandal, W. Urban | Coulex | 8 |
| 11 | A ~ 180 | ²³⁸ U, ²⁰⁸ Pb | Z. Podolyák | Coulex | 6 |
| 12 | ^{185,186,187} Pb | ²³⁸ U | J. Gerl, A. Andreyev G.D. Dracoulis | 2 step fragmentation lifetime | 8 |

Annex

- A1** *Shape evolution in light n-rich nuclei*
- A2** *Isospin symmetry and Coulomb effects towards the proton drip-line*
- A3** *Gamma-decay of the GDR in the exotic nucleus ^{68}Ni excited via Coulomb excitation*
- A4** *New shell structure at $N \gg Z$ – Relativistic Coulex in $N=28-34$ and $N=40-50$ nuclei*
- A5** *Investigation of the origin of mixed-symmetry states using relativistic Coulex on $N=52$ isotones*
- A6** *Relativistic Coulomb excitation of nuclei near ^{100}Sn*
- A7** *Nuclear magicity at $Z \sim 28, 50$ $N \sim 40, 82$ investigated through knock-out reaction of ^{132}Sn*
- A8** *Coulomb excitation at intermediate energies – Angular distribution and particle- γ angular correlation measurement*
- A9** *Magnetic moments of xenon and tellurium isotopes near doubly-magic ^{132}Sn at relativistic beam energies*
- A10** *Search for stable octupole deformation in neutron rich $^{142-144}\text{Ba}$ using Coulomb excitation*
- A11** *Prompt gamma spectroscopy and isomer tagging. Deformation of five-quasiparticle states in the $A \approx 180$ mass region*
- A12** *Investigation of the structure and deformation of $^{185-187}\text{Pb}$ by γ -spectroscopy and lifetime measurements*
- B1** *List of collaborating institutions*

Shape evolution in light n-rich nuclei

P. Mayet, et al.

Univ. Leuven

J. Gerl, Y. Kopach, S. Mandal, H.J. Wollersheim et al.

GSI, Darmstadt

F. Azaiez, et al.

IPN, Orsay

and the RISING collaboration

The light n-rich isotopes between the N=20 and N=28 shell closures provide an interesting testing ground for the shell model where drastic shape changes and co-existence of deformed and spherical structures are expected. One example is ^{32}Mg with a prolate deformation of the 2^+ state of $\beta \approx 0.5$ [1]. Recent theoretical work [2] predicts an even stronger deformation for ^{34}Mg and reduced deformation for ^{36}Mg . The aim of the proposed experiment is to study the level structure of nuclei in this mass region and, in particular, to determine for the first time lifetimes of excited states. B(E2)-values obtained from the lifetimes will be a measure of the deformation of the nuclei in their excited states.

Beam cocktails of excited nuclei with A/Z ratios between 2.5 and 3.0 can be well produced either by primary fragmentation [3] of a ^{48}Ca beam or by secondary fragmentation [4] of e.g. a ^{38}Si beam derived from fragmentation of the primary ^{48}Ca beam. The advantage of a two step process is that the intermediate beam produces in the second step the isotopes to be studied with a relative abundance in the cocktail which is 3 to 6 orders of magnitude higher than the production in one step. Thus detector load and background from unwanted channels is strongly reduced. The number of useful intermediate beams is of course limited since they have to be produced with a yield of 10^3 to 10^5 ions/s to be efficient.

The intermediate (respectively primary) beam will be selected by the first two sections of the FRS. The final fragmentation will take place with a target at the middle focus S2. The final fragments will be selected and identified by the further FRS sections and the standard S4 tracking detectors. The γ -decay of low energy low and medium spin states of the excited secondary fragments will be detected by segmented Clover detectors at forward and backward angles around the secondary target. The target-detector distance will be chosen to obtain an energy resolution of about 1% for a fragment energy of about 100 MeV/u. To determine lifetimes the target will be composed of a stack of three 0.3 g/cm^2 ^{197}Au foils, separated by 0.7 mm and 2.1 mm from each other. This arrangement results in specific γ -line shapes for lifetimes between about 0.1 ps and 20 ps covering the range expected for the nuclei of interest.

To reach the very n-rich nucleus ^{36}Mg a ^{48}Ca primary beam is necessary producing ^{38}Si as intermediate fragment. If this beam is available two settings of the FRS are planned. The first one employs the ^{48}Ca directly with an intensity of $10^5/\text{s} \dots 10^6/\text{s}$ (depending on the rate capability of the tracking and γ -detectors at S2). In the second setting a ^{38}Si intensity of $\approx 10^3/\text{s}$ is expected for a primary intensity of $10^9/\text{s}$ ^{48}Ca . With these two settings the whole range of Mg nuclei with $A=28..36$ will be reachable in the experiment. If a ^{48}Ca beam would not be available ^{50}Ti could be used instead. However, in that case the selected secondary beam would be ^{36}Si and ^{34}Mg would be the heaviest isotope. Beside the Mg isotopes the neighbouring isotopic chains is present in the fragmentation cocktail with similar intensities. Therefore the whole region of the nuclidic chart will be investigated with the two settings.

Using two Vega and four Exogam clover detectors at forward and backward angles a γ -detection efficiency of about 1% (at 1.3 MeV) can be achieved. Thus to obtain a minimum of 100 counts in the 2^+ γ -line 6 shifts of beam time are required for the direct fragmentation setting and 15 shifts for the secondary fragmentation setting.

- [1] T. Motobayashi et al., Phys. Lett. B346 (1995) 9.
- [2] H. Lenske, private communication, Univ. Giessen.
- [3] M. Belleguic, Ph.D. thesis, Univ. Lyon, 2000.
- [4] S. Wan et al., Eur. Phys. J. A6 (1999) 167.

Isospin Symmetry and Coulomb Effects Towards the Proton Drip-Line

M.A.Bentley, C.Chandler

School of Chemistry and Physics, Keele University, Staffordshire, ST5 5BG. U.K.

C.J.Barton, D.T.Joss, R.Lemmon, J.Simpson, D.D.Warner,
CLRC Daresbury Laboratory, Daresbury, Warrington, WA4 4AD. U.K.

R.Wadsworth

Department of Physics, University of York, Heslington, York YO10 5DD, UK.

D.Rudolph, C.Fahlander

Department of Physics, Lund University, S-22100 Lund, Sweden

W.Gelletly, Z.Podolyak, P.H.Regan

University of Surrey, Guildford, Surrey, GU2 7XH. U.K.

And the **RISING Collaboration**

(Gesellschaft für Schwerionenforschung, P.O.Box 110552, D-64291 Darmstadt, Germany)

Abstract

This proposal is aimed at the study of isobaric analogue states in light nuclei with a large proton excess and the use of the inherent isospin symmetry as a probe of detailed nuclear structure as the proton drip-line is approached. The principal aim of the proposal is to identify the lowest energy (yrast) structure of $T_z = -3/2$ nuclei in the $A=50$ region for the first time and, through comparison with their $T_z = 3/2$ mirror partners, to interpret the resulting Coulomb energies in the context of the nuclear shell model. Spectroscopic studies of these extremely proton-rich systems are generally beyond the scope of the usual techniques using fusion-evaporation reactions with intense stable beams. However, the fragmentation reaction has been shown to be capable of producing such exotic nuclei with manageable cross-sections *and* at reasonable angular momenta. The development of the RISING spectrometer now affords a unique opportunity to perform in-beam gamma-ray spectroscopic studies towards the proton drip-line using the secondary-fragmentation technique. The nuclei to be investigated are the $N=Z-3$ systems ^{45}Cr and ^{53}Ni .

1. Background and Physics Motivation

The investigation and understanding of fundamental symmetries is one of the principal goals of nuclear structure physics. One of the most basic of these is isospin symmetry – the exchange symmetry between the neutrons and protons in the nucleus - which arises because of the charge independence of the nuclear force. Excited states of the same total isospin, T , in a set of isobars have nearly degenerate values of excitation energy, with small differences attributable to Coulomb effects. The small differences in excitation energies (Coulomb energy differences, CED) between these isobaric analogue states can be associated with the subtle influence on the Coulomb force of the changing nucleon orbitals which contribute to the wave functions of the excited states. The study of this phenomenon, although still in its infancy, has shown some remarkable recent results and which help provide the motivation for the proposed experiment.

Recently, advances in experimental techniques have allowed the detailed spectroscopic investigation of $N=Z\pm 1$ mirror pairs in the $f_{7/2}$ -shell [1-4] up to high angular momenta. The evolution of the CED as a function of spin has revealed some remarkable effects. It has been found that the trends of the CED as a function of spin and energy can be understood *quantitatively* in terms of quite subtle nuclear structure effects – such as two-particle (rotational-) alignments, deformation changes and changes in the mechanisms by which the

nucleus generates angular momentum. Figure 1 shows a typical CED curve for the $A=49$ mirror pair $^{49}\text{Mn}/^{49}\text{Cr}$ [1] where the major variations in the CED have been successfully interpreted in terms of proton two-particle alignments, which result in changes in the spatial overlap of the proton wave functions. From studies such as this, it has now become clear that measurement of Coulomb effects as a function of spin can yield extremely valuable and very specific information on the details of the spatial behaviour of nucleons and nucleon-correlations within the nuclear potential.

Nuclei in this mass region are accessible to large-scale pf -shell model calculations [5]. This model has been extended to include the Coulomb interaction, and consequently CED predictions are now obtainable. The CED data thus provide a *uniquely* stringent test of the model on a state-by-state basis, and comparisons with the model are already yielding new insights into the capabilities of the shell-model approach (e.g. [2,3,6]).

A greater experimental challenge is the study of multiplets with larger total isospin, T . Very recently spectroscopy at high spin of even-even $T=1$ ($T_z=\pm 1$) mirror nuclei with $A=50$ [6] and $A=46$ [7] has been achieved for the first time, by identifying gamma decays in the most proton-rich ($N=Z-2$) isobars. The CED between these $T=1$ mirror states again showed that a very detailed understanding of the spatial correlations of pairs of particles can be gained. In these cases, it was also found necessary to include “one-body” effects in order to understand the CED. One such effect [6] is the Coulomb energies associated with nucleon orbitals of different radii, the occupation of which evolve as a function of spin, resulting in a contribution to the CED. These $A=46$ and $A=50$ even-even mirror nuclei described above represent the largest value of total isospin, T , for which isobaric analogue states have been studied at high spin.

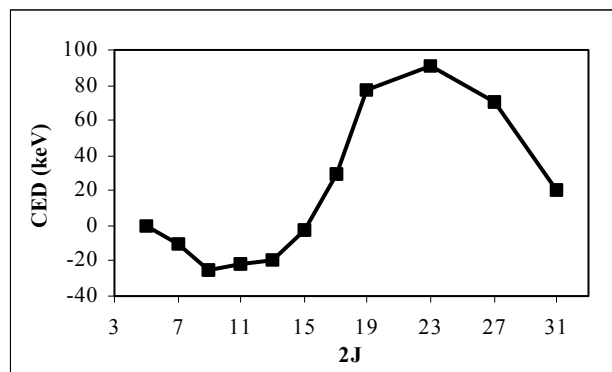


Figure 1: The Coulomb Energy Difference (CED) for the $^{49}\text{Mn}/^{49}\text{Cr}$ mirror pair [1]. The large rise at $J\sim 19/2$ is attributed to the rotational alignment of a pair of $f_{7/2}$ protons in ^{49}Cr , and the drop at higher spins is associated with the later alignment of $f_{7/2}$ protons in ^{49}Mn as the band termination is approached.

For mirror nuclei with larger values of isospin ($T\geq 3/2$) no detailed spectroscopic studies in medium-mass nuclei have been undertaken to date. Thus, the degree to which isospin symmetry holds (and hence our ability to interpret CED) as the proton drip line is approached remains an open question. For example, the large proton excess for the proton-rich members of these isobaric multiplets may be expected to have an increasingly significant effect on the one-body part of the measured Coulomb energy. This includes the bulk Coulomb effect associated with the differences in radii of specific orbitals as well as the more subtle effect of the Coulomb distortion of the specific nucleon wave functions (the Thomas-Ehrman shift). An indication that phenomena such as this may be important as the drip-line is approached can be found in the $N=Z$ odd-odd nucleus ^{70}Br [8]. Here the CED between the $T=1$ states and those in the neighbouring analogue nucleus ^{70}Se shows anomalous behaviour which has been interpreted in terms of the Thomas-Ehrman shift.

To date, the heaviest $T_z=-3/2$ nuclei for which excited states have been observed are to be found in the sd -shell (e.g. ^{29}S , see [9]), where one or two excited low-spin non-yrast states are known from transfer reactions. Thus there are no data that show how the CED evolves with increasing spin, and no information at all on excited states for $T_z=-3/2$ nuclei above $A=33$. In this work, we propose to study nuclei in the $f_{7/2}$ -shell – specifically the *even* Z , $T_z=-3/2$ nuclei (the *odd* Z , $T_z=-3/2$ systems all have very low proton separation energies, and the excited states are therefore likely to be particle-unbound). It is important to determine how the Coulomb effects to be investigated will evolve with mass across the single- j $f_{7/2}$ shell and, thus, in this work we will concentrate on ^{45}Cr and ^{53}Ni – located in different regions of the shell. The mirror nuclei of ^{45}Cr and ^{53}Ni (i.e. ^{45}Sc and ^{53}Mn) are well known, with low spin yrast structures that are well described by pure $f_{7/2}$

configurations outside a closed ^{40}Ca shell. In this experiment we aim to make a spectroscopic study of the energy levels of the proton-rich $T_z = -3/2$ nuclei up to 3-4 MeV excitation energy. This would correspond to the first few excited states in the yrast structures of the chosen nuclei. Additionally, the reaction mechanism proposed may populate low-spin non-yrast structures that are only weakly populated in the fusion-evaporation technique, allowing a more complete study of the Coulomb effects. The mirror pair $^{53}\text{Ni}/^{53}\text{Mn}$ is of particular interest, as these nuclei have a very simple $(f_{7/2})^{-3}$ structure – neutron holes in ^{53}Ni and proton holes in ^{53}Mn . This allows for a comparison of the $(f_{7/2})^{-3}$ proton and neutron multiplets, and the CED between these will give new information on the Coulomb two-body matrix elements in the upper $f_{7/2}$ shell – a vital ingredient for the shell model calculations that can only be derived from experimental data.

The technique to be used, secondary fragmentation (see next section), has only very recently been investigated as a technique for pursuing spectroscopic studies of nuclei far from stability (see e.g. [10]). This technique has not yet been applied to such proton-rich systems, and the proposed experiment will provide an essential test of the effectiveness of this novel approach.

In summary, we propose to use the secondary fragmentation technique to study exotic proton-rich nuclei through gamma-ray spectroscopy. These experiments are aimed at performing detailed spectroscopy, for the first time, of medium mass nuclei with $N=Z-3$, to test our understanding of Coulomb effects at large proton excess, and to provide the most rigorous tests of the nuclear shell model.

2. Experimental Details

The nuclei in question will be populated by the secondary fragmentation technique. A beam of ^{58}Ni at 600 MeV/A from SIS will impinge on a ^9Be target at the entrance of the Fragment Recoil Separator (FRS). The FRS will be used to select and identify a fragment (or range of fragments) close to the nuclei of interest. Following the FRS, at the target position of the RISING array, the fragments, at an energy of ~ 120 MeV/A, will impinge on a second ^9Be target, where a second fragmentation reaction occurs producing a range of secondary fragments - including the nucleus of interest. Gamma decays from states populated in the second fragmentation event will be measured in the RISING detectors. The expected energies of the gamma-decays (based on the “mirror” transitions in the mirror-partners) are all above 500 keV, once the Doppler shift is accounted for, and have lifetimes that are sufficiently short to decay within the focus of the RISING detectors. The secondary fragments will be identified down-stream in the transmission Si detector (ΔE) and thick scintillator (E). In this mass region, the ΔE -E information is expected to give a unique identification of the secondary fragments. The gamma-ray events and the ΔE -E data will be correlated to produce a clean gamma-ray spectrum “gated” by the final fragment of interest. The low energy level scheme of the nucleus will be deduced from this spectrum, through comparison with the known energies of the equivalent transitions in the mirror nucleus. Such mirror-symmetry arguments have been successfully used to deduce level schemes in mirror pairs – (see e.g. [3]). The reaction process of the secondary fragmentation event (with a very few nucleons removed) is expected to directly populate a few quite low-lying energy levels (see e.g. [11,12]) in addition to electromagnetic feeding from higher-lying states. Therefore, although the mirror partner to each nucleus of interest is well known, the distribution of the total cross-section amongst the various levels is unknown. Thus, to aid the analysis, the mirror partners of the nuclei of interest will be populated using an equivalent (i.e. “mirrored”) reaction. The two gamma-ray spectra for the mirror pair will be compared and the level scheme of the proton-rich member of the pair deduced.

To estimate rates, we take ^{45}Cr as an example. To identify the energy of a gamma transition, we estimate that such a transition should have a few hundred counts in a photo-peak in the final gated spectrum. To determine a beam-time estimate we require 200-300 counts be observed in a gamma decay from a state populated (either by direct population or feeding from above) in 50% of the reactions leading to ^{45}Cr . We assume a 4gcm^{-2} ^9Be primary target and a 700mgcm^{-2} secondary ^9Be target (limited to keep straggling and velocity spread at acceptable levels). We assume a primary ^{58}Ni beam intensity of 10^9 s^{-1} , an FRS efficiency of 25% and a photo-peak efficiency of 3% for a 1.3 MeV gamma ray measured in RISING. The EPAX code has been used to predict the cross-sections in each of the fragmentation reactions. The largest cross-sections are obtained when the intermediate fragment is chosen to be ^{47}Cr or ^{46}Cr . Each of these choices yields a similar final production rate of ^{45}Cr of 0.15 s^{-1} . For the purpose of an estimate, if we assume that the FRS is optimised to select just one of these intermediate fragments, then the required intensity in a gamma-ray peak in ^{45}Cr is obtained in four 8-hour shifts. Due to the smaller cross-section for ^{53}Ni , this requires an estimated 12 shifts

for the same gamma-ray intensity, using either ^{55}Ni or ^{54}Ni as the intermediate fragment. If the higher mass intermediate fragment (i.e. ^{55}Ni and ^{47}Cr) is used then the estimated intensities at the focal plane of the FRS are 10,000 to 20,000 s^{-1} . Additionally, the set-up of the FRS may result in a more diverse cocktail of fragments – again resulting in a higher rate. Should these rates exceed the capabilities of the FRS tracking detectors, then these could be switched off if necessary (once the FRS settings have been established), as only the identification of the final product is needed for tagging the gamma decays of interest. We will use one shift to determine the best choice of intermediate fragment, based on the rates observed and the distribution of nuclides at the focal plane of the FRS. To obtain data on the neutron-rich mirror partners (^{45}Sc and ^{53}Mn) one shift is estimated to be sufficient for each of these, due to the larger cross-sections. Two further shifts are requested to facilitate the necessary changes to the FRS settings. A summary of the request is as follows:

| Nucleus of interest | Intermediate fragment | Number of 8-hour shifts |
|---------------------|--------------------------------------|-------------------------|
| ^{45}Cr | ^{47}Cr or ^{46}Cr | 4 |
| ^{45}Sc | ^{47}V or ^{46}Ti | 1 |
| ^{53}Ni | ^{55}Ni or ^{54}Ni | 12 |
| ^{53}Mn | ^{55}Co or ^{54}Fe | 1 |
| FRS setting changes | | 2 |
| FRS optimisation | | 1 |

TOTAL REQUEST = 21 SHIFTS

References

- [1] C.D. O'Leary *et al.* Phys. Rev. Lett. **79** (1997) 4349
- [2] M.A. Bentley *et al.* Phys. Lett. **B437** (1998) 243
- [3] M.A. Bentley *et al.* Phys. Rev. **C62** (2000) 051303
- [4] J. Ekman *et al.* Eur. J. Phys **A9**(2000) 13
- [5] E. Caurier *et al.* Phys. Rev. **C50**(1994)225
- [6] S.M. Lenzi *et al.* Phys. Rev. Lett. **87** (2001) 122501
- [7] P.E. Garrett *et al.* Phys. Rev. Lett. **87** (2001)132502
- [8] G. de Angelis *et al.* Eur. J. Phys **A12**(2001)51
- [9] P.M. Endt. Nucl. Phys. **A521** (1990) 1-830
- [10] K. Yoneda *et al.* Phys. Lett. **B499**(2001)233
- [11] A. Navin *et al.* Phys. Rev. Lett. **81**(1998)5089
- [12] J. Enders *et al.* Phys. Rev. **C65**(2002)034318

Gamma-decay of the GDR in the exotic nucleus ^{68}Ni excited via Coulomb excitation.

A. Bracco, G. Benzoni, F. Camera, S. Leoni, P. Mason, B. Million, O. Wieland, N. Blasi and M. Pignatelli, *University of Milano*

A. Maj, M. Kmiecik, W. Meczynski, J. Styczen, *Cracow*

T. Aumann, H. Emling, J. Gerl, H. Wollersheim, P. Reiter et al. *GSI*

G. de Angelis, A. Gadea, D. Napoli, *LNL*

S. Lenzi, F. Della Vedova, E. Farnea, S. Lunardi, *Padova*

C. Petrache and G. Lo Bianco, *Camerino*

M. Castoldi and A. Zucchiatti, *Genova*

G. La Rana, *Napoli*

F. Azaiez, *Orsay*

Abstract

The proposed experiment aims at the investigation of the gamma-decay from the giant dipole resonance in the unstable neutron rich ^{68}Ni nucleus. To excite the giant dipole resonance use will be made of the Coulomb excitation in inverse kinematics of the beam of ^{68}Ni at 400 MeV/u on a ^{208}Pb target. For the ^{68}Ni nucleus calculations (in non-relativistic and relativistic random phase approximation) predict a “pygmy” component of the dipole response, namely a low-lying dipole strength (at energy below 10 MeV) which is much stronger than that of the less neutron rich stable isotopes. The investigation of the pygmy dipole resonance is interesting not only to study mean field modifications induced by large isospin in the ground state but also for its implications in the astrophysical models predicting the element abundances in the r-process.

For this experiment use will be made of both the RISING array at forward angles together with large volume BaF_2 detectors at the backward angles.

With 7 days of beam time we expect to measure with good statistics the pygmy part in the Ge detectors and the entire GDR response function with the BaF_2 detectors, being the main goal of the experiment. In addition, for the coincidence of high energy gamma-rays with the first 2^+ state we expect approximately 500 counts.

MOTIVATION

Giant resonances are basic nuclear excitation modes which carry useful information on the underlying nuclear structure as well as on the effective nucleon-nucleon interaction in the medium. Although this topic has attracted much attention over several past decades, in the case of nuclei far from the stability line the investigation of collective modes is still in its infancy.

The isovector giant dipole resonance (GDR) is one of the most important and easily accessible of these collective modes. The question how the giant dipole resonance strength evolves when going from stable to exotic, weakly bound nuclei with extreme neutron to proton ratio is presently under discussion [1-3]. The general feature of the existing calculations of different types, is the redistribution of the strength towards lower excitation energies well below the giant resonance region. The details of these redistribution are found to depend on the effective forces used in the calculations [3].

In the literature the low-energy part of the GDR strength function is often referred to as Pygmy resonance and it was proposed to arise from the vibration of the less tightly bound valence neutrons against the residual core.

Therefore measurements of the GDR strength function in unstable nuclei provide important information on the isospin dependent part of the in medium nucleon-nucleon interaction and on dipole type vibrations of the excess neutrons.

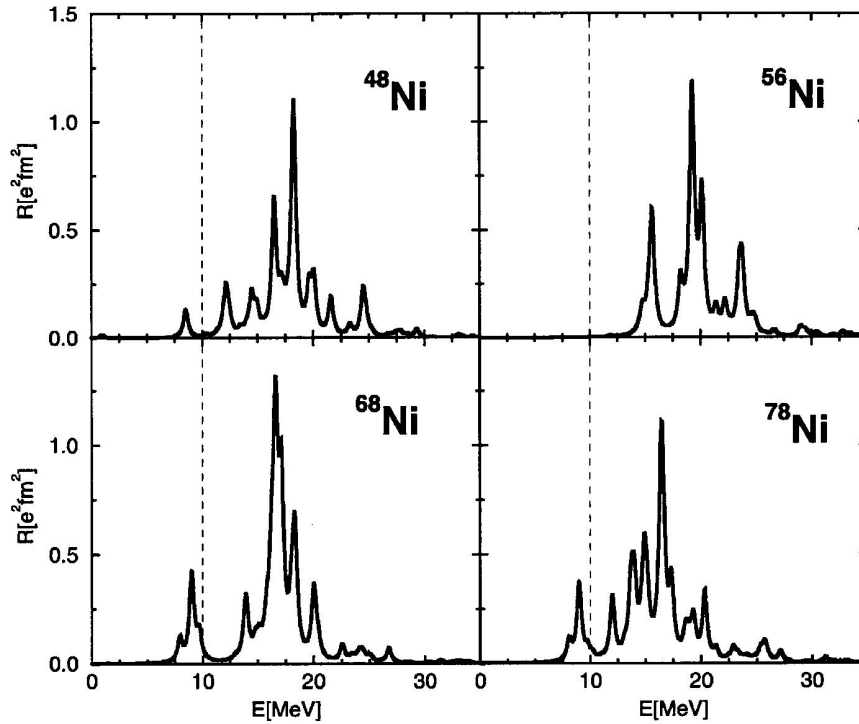


Fig. 1 The isovector dipole strength distribution for 4 different isotopes of Ni nuclei as predicted by D. Vretnar et al. using the Relativistic Random Phase Approximation approach. The dashed line is to separate the region of the giant resonances from the low-energy region below 10 MeV (pygmy region).

So far systematic experimental information on giant resonances in exotic nuclei is still not available and only for some light halo nuclei the low-lying dipole strength was observed in electromagnetic dissociation measurements, the heaviest among them being the neutron rich Oxygen isotopes recently investigated at GSI [4]. In these experiments the process of electromagnetic excitation (virtual photon absorption) of fast projectiles by a high Z target is used and the excitation energy is reconstructed from the break-up fragments and the neutron.

However, there is another method to study the GDR response function via relativistic Coulomb excitation, namely that of the virtual photon scattering. In this case one needs to detect the γ -ray decay which is a weak branch (at most of the order of a few percent)

from the GDR. It should be noted that the two methods are independent from each other and thus allow for a cross checking and that the gamma measurement may provide better resolution, i.e. may allow to resolve fine structures. In addition the gamma-branching ratios carries additional information.

Until now the virtual photon method has been used in experiments performed at MSU on ^{11}Be and ^{20}O beams at bombarding energies of 77 MeV/u and 100 MeV/u, respectively.

Results of these experiments (both performed with approximately 10^6 pps), are reported in references 5 and 6. The case of ^{11}Be , for which data were collected using BaF_2 detectors with energy up to $E_\gamma \approx 25$ MeV [5,7] (in coincidence with the elastically scattered ^{11}Be particles detected in a ΔE -E Plastic Phoswich array), can be taken as a good example to illustrate the feasibility of this type of measurements. In the MSU experiment on ^{11}Be it was possible to measure the entire GDR strength function and the root mean square charge radius was deduced. It was found that the charge distribution of ^{11}Be is similar to that of ^{10}Be core.

From both the existing studies on ^{11}Be and ^{20}O it is clear that the GDR γ -decay measurements following Coulomb excitation can be made more easily in the case of heavier neutron rich nuclei and at higher bombarding energies. This is because of the rapid increase of the excitation cross section with beam energy and charge. In fact, at a given Z the GDR excitation function increases by approximately one order of magnitude by going from 80 MeV/u to 400 MeV/u, the latter bombarding energy being available at GSI.

A neutron rich nucleus in the medium mass region which is very interesting for the study the GDR is ^{68}Ni . The energy of the first 2^+ state (2.03 MeV) and the corresponding $B(E2)$ value were measured showing a rather interesting interplay between shell closure and superfluidity at $N=40$ [8]. Recently Vretenar et al. [9] have applied the relativistic random phase approximation to predict the evolution of the isovector dipole response in nuclei with a large neutron excess. Their results for the case of the medium-heavy Ni isotopes are shown in figure 1. The low-energy dipole states built on valence neutron particle-hole configurations appear only on ^{62}Ni and on heavier isotopes. The relative contribution of the low-energy region ($E < 10$ MeV) to the dipole strength distribution increases with the neutron excess. In particular, the ratio of the energy weighted moment in the low-energy region ($E < 10$ MeV) and in the high-energy region ($E > 10$ MeV) is predicted to be of the order of 8%. Similar results have been obtained by Colo' et al. using the non relativistic Random Phase Approximation approach, which was first applied to the case of Oxygen isotopes [3].

In the case of ^{68}Ni isotopes it was found that in the region up to ≈ 10 MeV there is $\approx 7\%$ of the EWSR (similar values were found in break-up experiment for light nuclei). The details of these calculations, focussing on the pygmy part in the low-energy region are shown in figure 2.

It is important to point out that the knowledge of the low-lying dipole strength (pygmy resonance) in medium mass neutron-rich nuclei is relevant for astrophysical studies such as the calculations of the element abundancies in the r-process of the nucleosynthesis as reported in [10].

We have calculated the Coulomb excitation cross section using the theory of Winther and Alder reported in reference [11]. For the region above 10 MeV and centered at ≈ 15 MeV the expected cross section is 600 mb, while in the region of the pygmy resonance (8-10 MeV) the expected cross section is 150 mb. For the evaluation of the gamma decay branch from the resonance we have assumed a value of $\approx 2\%$. This last estimate is based on the experimental and theoretical work made for the GDR on the ^{208}Pb nucleus (see reference 12). In that work it was taken into account both the direct decay probability of the giant-resonance doorway state and the statistical decay probability of the underlying compound-nuclear levels.

The gamma-decay from the GDR to the low-lying 2^+ state depends on the details of the structure of this state. Presently calculations (within the quasi particle phonon model) and data are available only for the stable Sn isotopes and in that case the decay to the 2^+ state was found to be from 20 to 50% of that of the decay to the ground state [13].

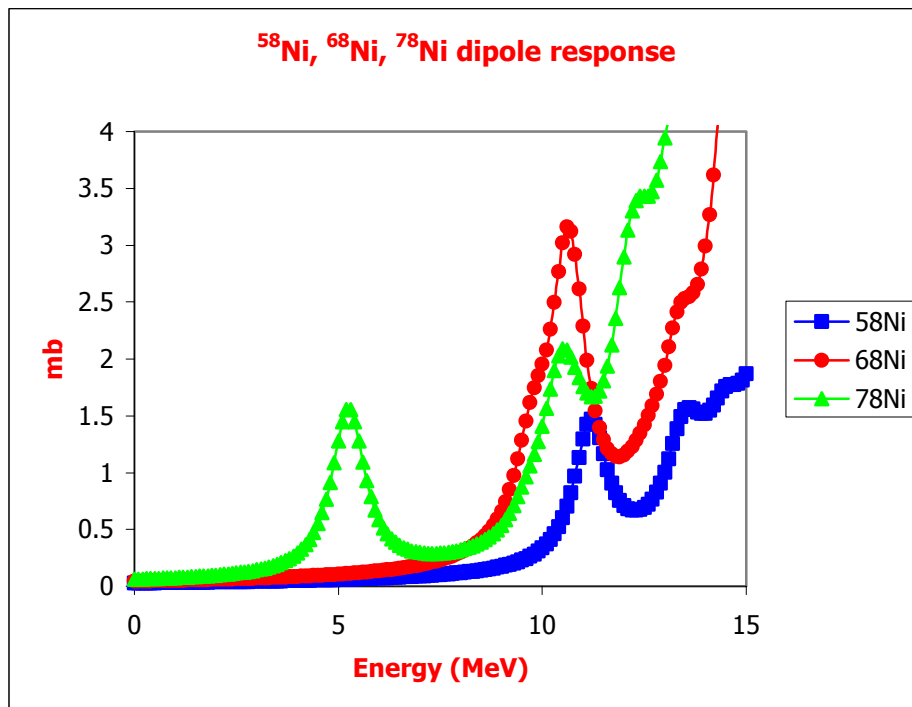


Figure 2. Photo absorption cross section in the low energy part of the dipole response calculated as in ref [3] for Ni isotopes. The calculation for ^{68}Ni is shown with filled circles. The entire strength function in the case of ^{68}Ni (the one which is planned to be measured) is in figure 3.

As a concluding remark it is important to stress that the availability of rather intense neutron rich beams at high bombarding energy together with the RISING facility makes GSI rather unique for the study of gamma-decay from the Coulomb excited Giant Dipole Resonance.

Experimental details

The experiment will be performed using a ^{68}Ni beam at a bombarding energy of 400 MeV/u impinging on a ^{208}Pb target with a thickness of 2 gr/cm^2 . The particle identification capability of the beam tracking before and after the interaction point is at the present energy and mass region sufficient to identify inelastic scattering events characterized by the same mass for the ejectile and projectile. The gamma decay from the giant dipole resonance region is expected to populate most strongly the ground state

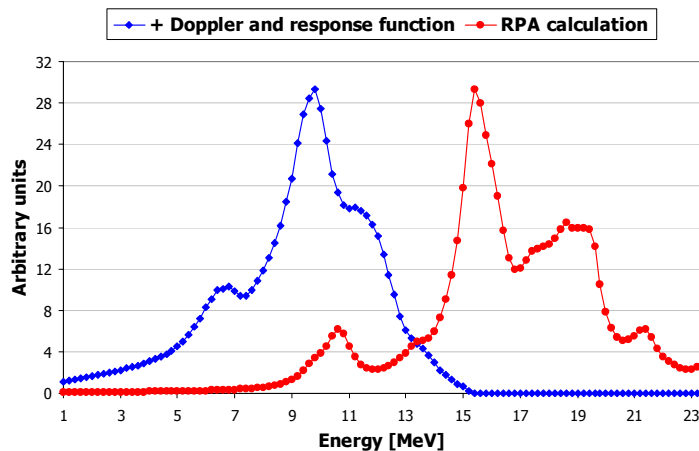


Fig. 3 Effect of the detector response function of BaF_2 positioned at backward angles on the GDR strength function. The curve extending at the highest energy is the photoabsorption cross section as predicted by the RPA calculation of G. Colo' et al. The curve at lower energy was obtained starting from the RPA calculation and applying the response function of the BaF_2 detectors at the backward angles.

but also the low-lying 2^+ state at 2.03 MeV.

Because of large Doppler shift we expect to be able to measure with the RISING Ge detectors only the pygmy part of the resonance (gamma rays of 10 MeV will be shifted to the energy of 17 MeV when emitted by the fast moving ^{68}Ni nuclei at 400 MeV/u, corresponding to $\beta=0.51$).

In contrast, the BaF_2 scintillators placed at the backward angles will detect the shift down gamma-rays and with those detectors one expects to be able to measure the entire dipole response function.

In order to choose the geometry of the BaF_2 detector system we have simulated the response of these detectors at the various angles not covered by the Ge cluster detectors. For the final choice of the angles it was taken into account that by going at backwards angles the emission from the target can be separated from that of the projectile. In fact, in that case the emission from the moving source is shifted at lower energies in a region of spectrum separated from that where the target emission is important. (at 13.5 MeV). The emission from the ^{208}Pb target is at rest being characterized by a GDR strength function

with a centroid at 13.5 MeV and a total width of 4 MeV. With the present choice of the geometry and beam energy is expected to be separated from the emission of the projectile. However, by measuring the gamma-rays in two BaF₂ detectors placed at 90° we expect to be able to subtract the remaining small contribution from the target emission in the region of the ejectile decay. The expected relativistic effects of the gamma emission combined with that of the response of the BaF₂ detectors are illustrated in figure 3. In that figure two different curves are displayed. One is the predicted GDR strength function for ⁶⁸Ni, while the other is obtained by folding the detector response function (calculated with the code Geant) and the relativistic Doppler effects. One can note that the pygmy part of the GDR response function becomes rather compressed. The opposite situation is instead expected in the case of the gamma emission as detected with the Ge cluster detectors at the forward angles. The Ge detectors are therefore better suited for the study of the pygmy part of the dipole response particularly because the calculations predict a rather narrow structure. The detection efficiency for the pygmy structure (which will be shifted at 16-17 MeV) was calculated to be 0.4 % .

With seven days of beam time we expect to obtain 1.8*10⁴ counts in the BaF₂ detectors (about 400 counts in each 0.2 MeV bin) and 1600 counts in the pygmy part in the Ge detectors. For the coincidence between the high-energy gamma-rays with the low-energy gamma-rays from the first 2⁺ state we expect 500 counts.

In the appendix below all the details concerning the count rate estimates are given.

APPENDIX : estimate of the expected rates.

Beam intensity : To produce ⁶⁸Ni use the fragmentation reaction of ⁸⁶Kr on ⁹Be target.

The cross section σ is $5.4 \cdot 10^{-5}$ barn

Primary beam intensity of ⁸⁶Kr : $1 \cdot 10^{10}$ particle/sec

⁹Be target thickness 1 g/cm² (corresponding to $6.7 \cdot 10^{22}$ atoms/cm²)

Luminosity L ((number of beam particles) /s * (target atoms)/cm²)
 $= 6.7 \cdot 10^{32}$

Secondary beam intensity = $L \cdot \sigma = 3.6 \cdot 10^4$ particles/s

Transmission SIS-FRS = 70%

Beam on the secondary target = $2.5 \cdot 10^4$ particles/s

(Note that the same calculation made for the fragmentation of ⁸⁶Kr on ²⁰⁸Pb gives for the intensity of the beam on the secondary target = $2.7 \cdot 10^3$ particles/s)

Secondary target thickness : 2g/cm²

Coulomb excitation cross section = 600 mb (in the region at high energy)

Coulomb excitation cross section = 150 mb (in the region of the pygmy)

Efficiency of BaF₂ (at 10 MeV) = 1.1 %

Efficiency of RISING at 15 MeV = 0.4 %

Gamma- decay branch : 2%

Efficiency to detect the 2.03 MeV state in the combined system Germanium + BaF₂ Detectors : 5 %.

Counts/day in the interval 5-13 MeV = 2514 Counts per day in the BaF₂ detectors (about 60 counts in each 0.2 MeV bin).

Counts/day in the interval 15-17 MeV in the germanium detectors (Forward shifted pygmy part) = 230 counts per day.

Counts in coincidence with 2⁺ state : 70 per day.

References

- [1] H. Sagawa, T. Suzuki, Phys. Rev. C59(1999)3116
- [2] F. Ghielmetti, G.Coló, P.F. Bortignon, R.A. Broglia, Phys. Rev. C54(1996) R2143.
- [3] G. Coló and P.F. Bortignon, NPA696(2001)427.
- [4] T. Aumann et al, NPA687(2001)103c.; A. Leistenschneider et al. PRL86(2001)5442.
- [5] R.L. Varner et al., Proceedings of the international Workshop on Collective Excitation in Fermi and Bose Systems, edited by C. Bertulani, World Scientific (1999)264.
- [6] E. Tryggestad et al., NPA687(2001)231c.
- [7] A. Bracco, slides from the RISING Workshop, 6-april 2001, www-aix.gsi.de/~wolle/EB_at_GSI/FRS-WORKING/main.html
- [8] F. Azaiez, Physica Scripta T88(2000)118 and O. Sorlin et al. PRL88(2002)092501.
- [9] D. Vretenar et al., NPA692(2001)496.
- [10] S. Goriely, Phys. Lett. B 436(1998)10.
- [11] Winther and Alder, NPA319(1979)518.
- [12] A.M. Nathan, PRC43(1991)R2479 and references therein.
- [13] V. Yu Ponomarev et al, NPA550(1992)150.

New shell structure at $N \gg Z$ – Relativistic Coulex in $N=28-34$ and $N=40-50$ nuclei

A RISING proposal

H. Grawe¹, M. Górska¹, J. Döring¹, C. Plettner¹, NN, C. Fahlander², NN, H. Hübel³,
A. Neusser³, P. Bringel³, A. Bürger³, P. Reiter⁴, NN

¹ *Gesellschaft für Schwerionenforschung mbH, D-64291 Darmstadt, Germany*

² *Department of Physics, Lund University, Sweden*

³ *ISKP, University of Bonn, Germany,*

⁴ *IKP, University of Köln, Germany*

Abstract

It is proposed to measure the $I^\pi=2^+$ excitation energy and the $B(E2;0^+ \rightarrow 2^+)$ strength of neutron-rich Ca isotopes and $N=32,34$ isotones, Ni isotopes and $N=50$ isotones using relativistic Coulomb excitation at 100 A·MeV. The radioactive species will be produced, separated and identified by fragmentation of 750 A·MeV ⁸²Se and ⁸⁶Kr at the GSI SIS/FRS facility, and γ rays will be detected in the RISING fast-beam setup. The main goal of the project is the study of changing shell structure of n-rich nuclei around $N=28-34$ and $40-50$ via the aforementioned experimental signatures.

Spokespersons: H. Grawe, H. Hübel, P. Reiter

GSI contact persons: H. Grawe, M. Górska

1 Introduction and physics motivation

The development of new shell structure at $N \gg Z$ as studied in light and medium-heavy neutron-rich nuclei around $N=8,20,28$ [1, 2, 3] is generally ascribed to the weakening of the surface slope of the neutron potential due to the large neutron excess [4]. As a consequence the familiar Woods-Saxon (WS) shape of the potential for nuclei close to stability is expected to change towards a harmonic oscillator (HO) type. This goes along with a **reduction** of the spin-orbit splitting, which is proportional to the potential slope, and thus HO magic numbers are expected to be reinforced [4].

Alternatively, the existing experimental evidence of changing shell structure along the $N=8, 20$ and 28 isotonic sequences can be qualitatively explained in terms of the monopole part of the nucleon-nucleon residual interaction. Schematically this is due to the $(\sigma \cdot \sigma) (\tau \cdot \tau)$ part of the interaction, which is binding and strongest in the $S=0$ (spin-flip) and $T=0$ (proton-neutron) channel of the two-body interaction. This causes large monopole shifts of neutron single-particle orbits due to their missing $S=0$ proton partners at large neutron excess, and thus generates new shell gaps. The effect was first discussed recently for the sd shell [5, 6] and for the pf shell [6, 7]. The relevant regions of known and expected changes in shell structure are indicated in Fig. 1. It should be pointed out that the effect leads to an **increased** spin-orbit splitting.

2 Status and expected trends

The status and basic experimental features of shell structure at $N \gg Z$ for medium-heavy nuclei have been reviewed recently [7]. With respect to three typical signatures for shell structure they are summarized in Fig. 2 for the Ca and Ni isotopes and the $N=50$ isotones.

2.1 The $Z \simeq 20$, $N \simeq 34$ region

It is known experimentally [7] that the neutron $\nu f_{5/2}$ orbit from ^{57}Ni towards ^{49}Ca undergoes a large monopole shift due to the reduced binding with increasing removal of the proton $\pi f_{7/2}$ $S=0$ spin-orbit partners. Beyond $N=28$ this opens a gap between the $\nu(p_{3/2}, p_{1/2})$ and $\nu f_{5/2}$ orbits, which might be subject to change depending on the $2p_{1/2}$ position, as this also forms a $S=0$ pair with $\pi 1f_{7/2}$ but with less radial overlap. In Fig. 2 experimental signatures for shell structure, the two-nucleon separation energy differences δ_{2n}/δ_{2p} , the $I^\pi=2^+$ excitation energies $E(2^+)$ and the $B(E2; 2^+ \rightarrow 0^+)$ values are shown for several chains of isotopes and isotones [7]. In the Ca isotopes (Fig. 2a) beyond $N=28$ a possible (sub)shell closure at $N=32, 34$ seems to develop in $E(2^+)$. It has been reported out recently that the Cr isotopes show a maximum in $E(2^+)$ at $N=32$ [8]. On the other hand within the $N=34$ isotones $E(2^+)$ is increasing from Fe to Cr in contrast to the expected trend towards midshell, which supports a $N=34$ closure [8]. Besides masses, which due to short halflives are difficult to measure, obviously $E(2^+)$ and $B(E2)$ values for $^{50-54}\text{Ca}$ are missing for a proof of the concept. Similarly a study of the $N=30-34$ isotones of **Cr** and **Ti** would reveal such a change in shell structure.

2.2 The $Z \simeq 28$, $N \simeq 40-50$ region

The shell behaviour in this region is dominated by the monopole strength of the $\pi f_{5/2}$ $\nu g_{9/2}$ and $\pi f_{7/2}$ $\nu f_{5/2}$ pairs of nucleons, which is known from experiment [7, 9]. At $N=40$ ^{68}Ni as an isolated nucleus exhibits doubly-magic features, which rapidly disappear when adding protons into $\pi f_{5/2}$ or removing them from $\pi f_{7/2}$ as in both cases the gap between $\nu g_{9/2}$ and $\nu f_{5/2}$ is closed by increased $\nu g_{9/2}$ and decreased $\nu f_{5/2}$ binding, respectively. It is an interesting question whether this affects the $N=50$ shell at ^{78}Ni , too, where the $\pi f_{5/2}$ orbit is empty, which shifts $\nu g_{9/2}$ towards $\nu d_{5/2}$ (see Fig. 1).

The experimental evidence is scarce, indirect and partly contradictory. A reduced shell gap can be inferred from ^{80}Zn β -decay [10] and the existence of a $I^\pi=(5/2)^+$ ground state in ^{67}Fe [11]. On the other hand the $I^\pi=8^+$ $\nu g_{9/2}^2$ isomer found in ^{78}Zn has an almost identical $B(E2)$ strength as the corresponding one in ^{70}Ni [12], which seems to exclude a major $\nu g_{9/2}^{-1} d_{5/2}$ $E2$ polarisation. Whether the puzzling disappearance of the $I^\pi=8^+$ isomerism in $^{72,74}\text{Ni}$ [13] can be related to an admixture of this configuration to the $I^\pi=6^+$ state is an yet open question. Shell model calculations of the $B(E2; 2^+ \rightarrow 0^+)$ [14] have not treated excitations beyond $N=50$. An $E(2^+)$ and $B(E2; 0^+ \rightarrow 2^+)$ study of the $N=50$ isotones ^{84}Se and ^{82}Ge (Fig. 2c), $^{70-74}\text{Ni}$ (Fig. 2b) and $^{66,68}\text{Fe}$ will shed light on the development of shell structure in this region. In none of these cases a deformed structure can be excluded, as has been postulated for ^{66}Fe [15] (see also Figs. 2b,c).

3 Proposed experiments

We propose to study Coulomb excitation of the nuclei listed in Table 1 including calibration points. The radioactive isotopes are produced by projectile fragmentation at 750 A·MeV primary beam energy. Reaction products after slowing down to 100 A·MeV are Coulomb excited by a secondary Pb target. They are traced and identified in the FRS from the production target to the secondary target at S4, and after that the scattered products are identified in A and Z with a resolution of about 1%. The γ -rays from the deexcitation of Coulomb excited states emitted in-flight are detected in RISING.

4 Count rates and beam request

In Table 1 the nuclei to be studied are listed with their EPAX production cross section, corresponding RIB beam intensities, Coulomb excitation cross sections based on known and estimated $E(2^+)$ energies and $B(E2; 0^+ \rightarrow 2^+)$ values as deduced from Raman systematics [16]. The number of detected γ -rays per hour were calculated assuming a primary beam of 1×10^9 particles/s, a thickness of 2 g/cm² for the Be fragmentation and 1 g/cm² for the Pb Coulex targets, 20% FRS transmission and a γ -ray efficiency of $\epsilon_\gamma = 2.5\%$. We require a minimum count rate of 2/h in a 1 MeV $2^+ \rightarrow 0^+$ γ -ray. The most exotic and interesting cases in Table 1 require two beams, ⁸⁶Kr and ⁸²Se, the latter with two FRS settings. We therefore request **15 shifts** of ⁸⁶Kr and **24 shifts** of ⁸²Se, which includes time for FRS tuning and is mandatory to cover the most significant cases.

Table 1: Details of RIB intensities and γ -ray count rates

| RIB | Beam | A/Z | σ_{frag} barn | I_{RIB} 1/s | $E(2^+)$ MeV | $B(E2)$ WU | σ_{Coul} mb | N_γ 1/h | comment |
|------------------|------------------|------|-------------------------|------------------|-----------------|---------------|-----------------------|-------------------|-------------------|
| ⁵⁰ Ca | ⁸² Se | 2.50 | 4.5[-6] | 1.8[+2] | 1.03 | 15.6 | 250 | 7.8 | direct evidence |
| ⁵² Ca | ⁸² Se | 2.60 | 1.4[-7] | 5.7[0] | 2.56 | 0.58 | 10.3 | 0.01 | not feasible |
| ⁵⁰ Ti | ⁸² Se | 2.27 | 2.3[-3] | 9.2[+4] | 1.55 | 5.3(8) | 86 | 1380 | calibration |
| ⁵² Ti | ⁸² Se | 2.36 | 3.2[-4] | 1.3[+4] | 1.05 | 17.1 | 290 | 650 | direct evidence |
| ⁵⁴ Ti | ⁸² Se | 2.45 | 2.3[-5] | 9.2[+2] | 1.00 | 16.6 | 290 | 47 | direct evidence |
| ⁵⁶ Ti | ⁸² Se | 2.55 | 1.0[-6] | 4.0[+1] | ~1.25 | 12.4 | 230 | 1.6 | direct evidence |
| ⁵⁸ Cr | ⁸² Se | 2.42 | 1.0[-4] | 4.0[+3] | 0.88 | 19.5 | 366 | 255 | direct evidence |
| ⁶⁰ Fe | ⁸² Se | 2.31 | 2.7[-3] | 1.1[+5] | 0.82 | 13.3(25) | 260 | 4930 | calibration |
| ⁶⁶ Fe | ⁸² Se | 2.54 | 2.8[-6] | 1.1[+2] | 0.56 | 27.6 | 580 | 11 | indirect evidence |
| ⁶⁸ Fe | ⁸² Se | 2.62 | 1.5[-7] | 6.0[0] | ~0.50 | 29.1 | 630 | 0.6 | difficult |
| ⁷⁰ Ni | ⁸² Se | 2.50 | 4.0[-5] | 1.6[+3] | 1.26 | 12.6 | 290 | 80 | indirect evidence |
| ⁷² Ni | ⁸² Se | 2.57 | 2.5[-6] | 1.0[+2] | 1.10 | 13.7 | 320 | 5.5 | indirect evidence |
| ⁷⁴ Ni | ⁸² Se | 2.64 | 1.4[-7] | 5.7[0] | ~1.00 | 12.9 | 330 | 0.3 | difficult |
| ⁸² Ge | ⁸⁶ Kr | 2.56 | 8.7[-7] | 3.5[+1] | 1.35 | 11.2 | 290 | 1.7 | direct evidence |
| ⁸⁴ Se | ⁸⁶ Kr | 2.47 | 4.7[-4] | 1.9[+4] | 1.45 | 11.2 | 310 | 1030 | direct evidence |

References

- [1] A. Navin *et al.*, Phys. Rev. Lett. **85** (2000) 266
- [2] N. Orr *et al.*, Phys. Lett. **B258** (1991) 29
- [3] O. Sorlin *et al.*, Phys. Rev. **C47** (1997) 2941
- [4] J. Dobaczewski *et al.*, Phys. Rev. Lett. **72** (1994) 981
- [5] T. Otsuka *et al.*, Phys. Rev. Lett. **87** (2001) 082502
- [6] T. Otsuka *et al.*, Eur. Phys. J. **A13** (2002) 69
- [7] H. Grawe, M. Lewitowicz, Nucl. Phys. **A693** (2001) 116
- [8] J.I. Prisciandaro *et al.*, Phys. Lett. **B510** (2001) 17
- [9] S. Franchoo *et al.*, Phys. Rev. **C64** (2001) 054308
- [10] K.L. Kratz *et al.*, Phys. Rev. **C58** (1998) 278
- [11] M. Sawicka *et al.*, to be published
- [12] J.M. Daugas *et al.*, Phys. Lett. **B476** (2000) 213
- [13] H. Grawe *et al.*, Proc. TOURS 2000, AIP Conf. Proc., **CP561** (2001) 287
- [14] O. Sorlin *et al.*, Phys. Rev. Lett. **88** (2002) 092501
- [15] M. Hannawald *et al.*, Phys. Rev. Lett. **82** (1999) 1391
- [16] S. Raman *et al.*, ADNDT **42** (1989) 1

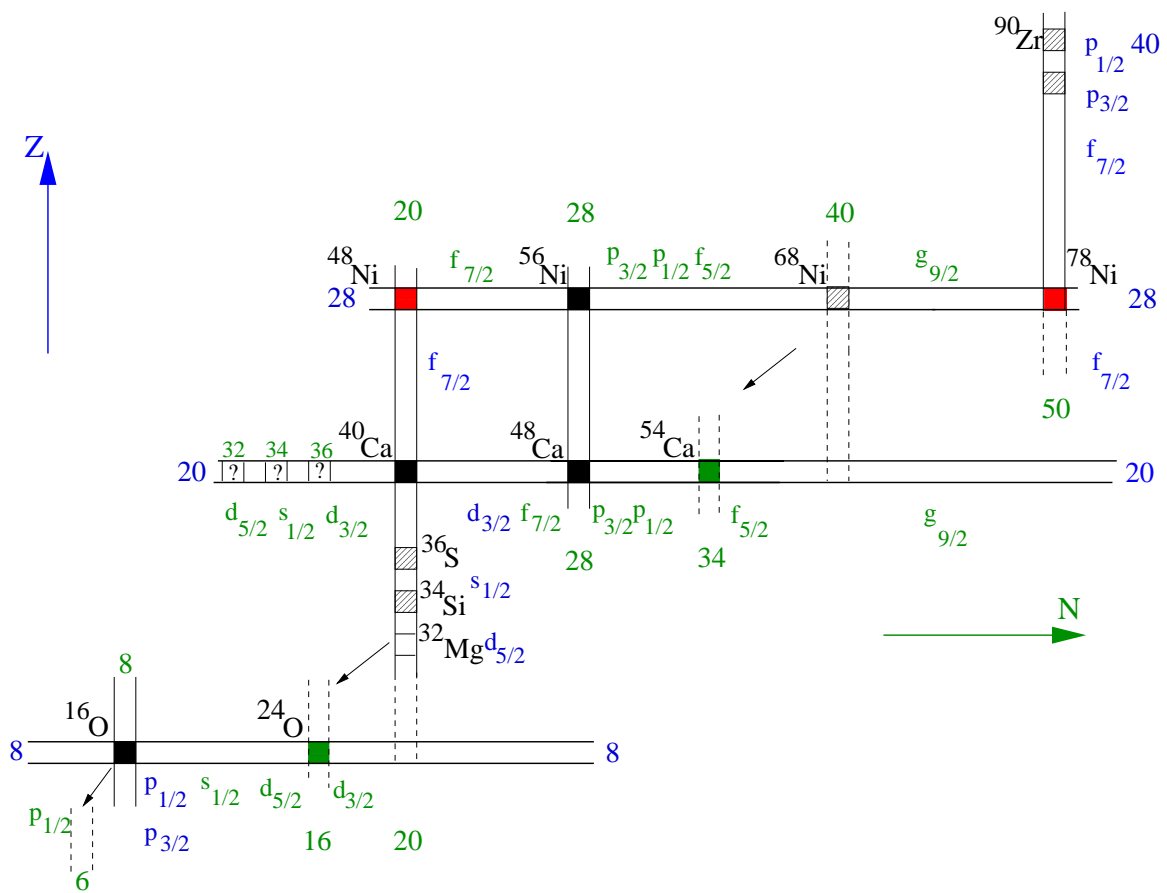


Figure 1: Schematic illustration of known and expected new shell structure in $N \gg Z$ nuclei

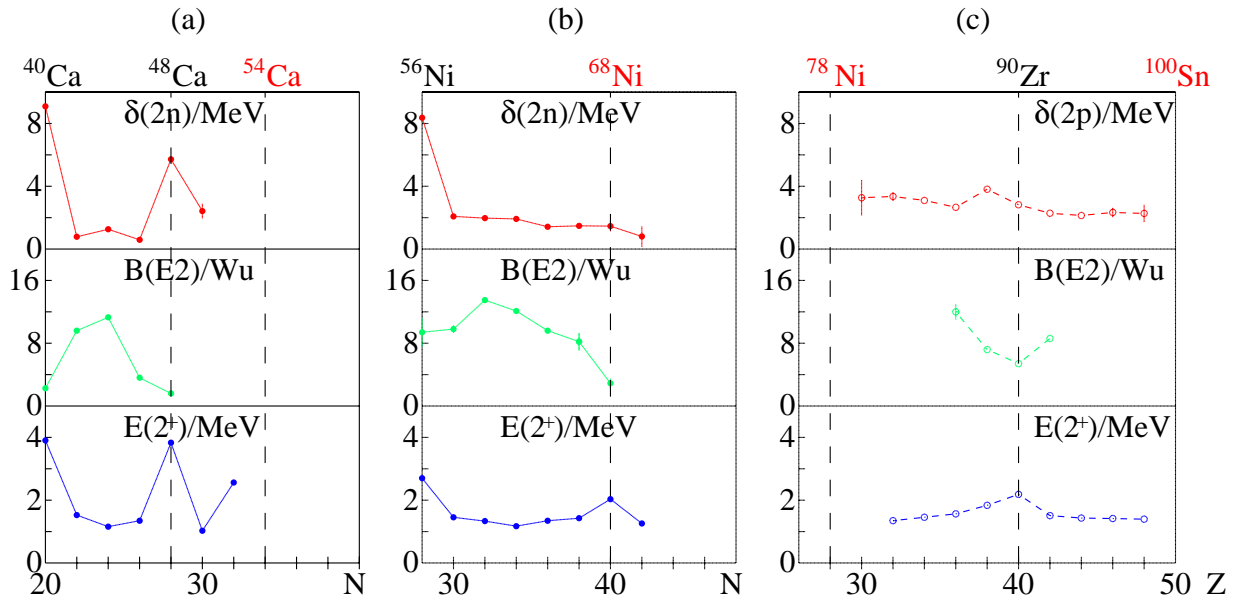


Figure 2: Excitation energy of $I^\pi=2^+$ states, E2 strengths $B(E2;2^+ \rightarrow 0^+)$ and the two-nucleon separation energy differences δ_{2n}/δ_{2p} for Ca (a), Ni (b) isotopes and the N=50 isotones (c)

Investigation of the origin of mixed-symmetry states using relativistic COULEX of N=52 isotones

D. Tonev^a, A. Dewald^a, C. Fransen^a, J. Jolie^a, A. Linnemann^a, A. Lisetskiy^a, M. N. Mineva^b, P. Pejovic^a, P. Petkov^{a,c}, N. Pietralla^a, V. Werner^a, and the RISING collaboration

^a Institut für Kernphysik der Universität zu Köln, 50937 Köln, Germany

^b Division of Cosmic and Subatomic Physics, Lund University, S-22100, Sweden

^c Bulgarian Academy of Sciences, Institute for Nuclear Research and Nuclear Energy, 1784 Sofia, Bulgaria

1 Introduction

The atomic nucleus with its two different constituents, protons and neutrons, represents a unique finite quantum many body system. The evolution of its properties can be investigated in detail by varying the finite number of protons and neutrons. One of the fundamental aspects of nuclear structure physics is the understanding of how collective quantum phenomena, such as deformation or phonon excitations, arise. From these studies one knows that proton-neutron correlations in the valence space play an important role in the formation of collective motion. However, possible combinations of protons and neutrons which could be studied in detail were up to now mostly limited to stable and proton rich nuclei. Important observables, needed for such studies, are lacking for nuclei on the neutron rich side of the nuclear chart.

In principle, the nuclear shell model represents the ideal theoretical microscopic tool to attack the problem of understanding the evolution of collective

nuclear structure. However, the description of collective excitations requires often a very large configuration space and, hence, model calculations must be truncated to appropriate valence spaces leading to necessary re-adjustments for the parameters of the effective residual interactions and single-particle energies. These effective model parameters must be obtained from experiment. The investigation of symmetries can help to gain a more detailed understanding of nuclear forces. The isospin symmetry represents one of the fundamental symmetries of nucleonic systems.

Recent nuclear structure studies address the detailed investigation of nuclear shell structure, in particular, at extreme values of isospin. Besides the studies of yrast excitations in very neutron rich nuclei another sensitive probe for the isospin-dependence of nuclear forces in the valence shell is represented by the properties of collective isovector valence shell excitations. Since shell model descriptions of collective structures often requires too big spaces it is useful to employ specific truncation schemes optimized for the description of the phenomena of interest.

The interacting boson model (IBM) [1] represents a kind of a truncated shell model appropriate for the description of quadrupole-collectivity. Besides its schematic character the IBM offers very useful insights into the nuclear structure revealing different symmetries of the nuclear wave functions. Because the Interacting Boson Model is based on nucleon pairs formed by either two valence neutrons or two valence protons, it allows also the study of proton-neutron correlations, albeit of nucleon pairs.

The framework of the IBM-2 extends the isospin formalism to the IBM boson systems. These bosons are considered to be “elementary” particles that form a doublet with projection $+1/2$ (proton boson) and $-1/2$ (neutron boson). In order to avoid confusion with the ordinary isospin for nucleons the “boson-isospin” is called F-spin. It should be also mentioned that the F-spin

in the IBM does not match the total isospin of corresponding valence nucleon pairs. However, formally, isospin and F-spin are complementary analogous. The former applies to “elementary” nucleons, the latter to “elementary” bosons.

For the description of a given nucleus with fixed numbers of proton and neutron bosons, N_π and N_ν , respectively, the z-component of the F-spin is a good quantum number, namely it is $F_z = N_\pi(1/2) + N_\nu(-1/2) = (N_\pi - N_\nu)/2$. For a given total boson number, $N = N_\pi + N_\nu$, the total F-spin quantum number can take values between F_z and $F_{\max} = N/2$.

The IBM predicts new entire classes of collective states with F-spin quantum numbers $F < F_{\max}$. Wave functions of such states contain at least one pair of proton and neutron bosons that is antisymmetric under the exchange of the proton and neutron labels. These states are called mixed-symmetry (MS) states. They are different from the low-lying collective states, which are symmetric with respect to the pairwise exchange of boson isospin labels.

In the mid-eighties a new collective $J^\pi = 1^+$ excitation, called scissors mode, was discovered in deformed gadolinium nuclei by A. Richter and collaborators [2]. Scissor states were subsequently observed in many deformed nuclei [3] and intensive theoretical studies of such states were done. The scissors mode was predicted [4] by the IBM as a one representative of the class of collective MS states in which valence neutrons and protons move out of phase.

According to the IBM approach the whole class of MS states is formed by quadrupole-collectivity. The building block of all MS excitations is, therefore, predicted to be the MS 2_{ms}^+ state, which should occur in spherical nuclei as the lowest, one-phonon MS state on which collective multiphonon structures can be built. The existence of such a multiphonon structure with MS character was recently discovered in the nuclide ^{94}Mo [5, 6, 7]. Recent measurements

on ^{94}Mo and other $N = 52$ isotones confirm [8, 9, 10] the initial findings as a general phenomenon.

2 Scientific motivation

The $N = 52$ isotones close to the $Z = 38, 40$ sub-shell closures correspond to sufficiently small valence spaces for a practical description of those nuclei in terms of the nuclear shell model. This fact offers the unique possibility to compare IBM calculations to shell model calculations and such to achieve a microscopic understanding of the building blocks of nuclear collectivity [11]. Moreover, the evolution of MS states in $N = 52$ isotones can be tracked over different proton shells enabling us to investigate the variation of the proton-neutron interaction as a function of the nuclear valence space. It is of great interest to study the cases with the smallest possible number of valence particles which are already able to induce the collective features. There we can apply the shell model to understand the generating mechanism of collectivity, the role of the proton-neutron interaction, to explore the microscopic origin of the symmetries in the IBM and to test the limits of application of the IBM.

Unfortunately, the light $N = 52$ isotones below $Z = 40$ are unstable neutron rich nuclei and, therefore, no data on absolute transition rates exist. Absolute electromagnetic transition rates and magnetic moments for low-lying states are, however, necessary information in order to uniquely identify MS states and are, therefore, the prerequisites for the systematical understanding of the proton-neutron non-symmetric building blocks of nuclear collectivity.

It is the aim of our proposal to study the quadrupole collectivity and to identify MS states in neutron rich $N = 52$ isotones by using relativistic Coulomb excitation. It was recently demonstrated that the process of

Coulomb Excitation in inverse kinematics is very well suited also for the population of one-phonon MS states [8]. The single step COULEX reaction will populate in a very clean way the excited 2^+ states and the $B(E2; 0_1^+ \rightarrow 2_i^+)$ transition strengths and large $B(M1; 2_i^+ \rightarrow 2_1^+)$ values can be deduced from the measured cross sections and branching ratios. These absolute transition strengths will then be used for comparison with detailed shell model and IBM calculations. They should allow us to obtain a microscopic understanding of the mixed symmetry states and their evolution with proton number.

The next questions arising from these studies are: How do symmetric and mixed symmetry structures evolve at $Z \leq 38$? What is the importance of different proton orbitals? How do single particle and collective motions interfere? How does the change in proton number influence the neutron configurations? And how good is the sub-shell closure at $Z = 38$ or $Z = 40$? Approaching the sub-shell at $Z = 38$, the nuclei ^{90}Sr (two neutrons outside the $N = 50$ closed shell), ^{88}Kr (two proton holes and two neutrons outside the closed shells), ^{86}Se (four protons holes and two neutrons), form an ideal testing ground to answer these questions. Since the neutron number $N = 52$ is the same in all these nuclei we could extend in a systematic way (see Fig. 1) our studies of ^{92}Zr [10], ^{94}Mo [5, 6, 7], and ^{96}Ru [8, 9]. The crucial point for this extension is a measurement of the $B(E2; 0_{g.s.}^+ \rightarrow 2_{1,2,3}^+)$ values (see also Fig. 1).

In order to check how good our experimental approach using relativistic Coulex would be, we shall investigate as reference nucleus ^{84}Kr to determine $B(E2; 0_{g.s.}^+ \rightarrow 2_{1,2,3}^+)$ values. It should be mentioned that the transition energies of $2_1^+ \rightarrow 0_{g.s.}^+$ of all three neutron rich nuclei of interest are well known (see also Fig. 1) - ^{84}Kr [13], ^{88}Kr [14] and ^{86}Se [15]. Theoretical calculations of energy spectra and transition strengths are also available [12] and it would be of considerable interest to compare these model predictions

with the new experimental data that we hope to obtain.

3 Experiment and preliminary calculations

Coulomb excitation is the excitation of a nucleus via the electromagnetic interaction with another nucleus [16]. The electromagnetic interaction between the projectile and target as well as the reaction mechanism of Coulomb scattering are well known [17].

We will use the standard RISING set up for relativistic Coulex experiments. We propose to use the fission of a 750 MeV/nucleon ^{238}U beam on a 1.0 g/cm^2 ^{208}Pb target in order to produce the neutron rich ^{90}Sr , ^{88}Kr , ^{86}Se nuclei. The primary beam intensity of ^{238}U is estimated to about $\sim 10^9$ particles per second. According to the calculations, the predicted cross section for the production of ^{88}Kr is 26 mbarns.

In order to estimate the Coulomb excitation cross sections we assume an energy of about 100 MeV/nucleon in a 0.4 g/cm^2 ^{208}Pb secondary target. The photopeak efficiency is about 0.029. According to the calculations we found a cross section for the Coulomb excitation of the first 2_1^+ state in ^{88}Kr with $E_\gamma = 775\text{ keV}$, $\sigma_{\text{Coul}ex} = 200\text{ mbarn}$. For the second 2_2^+ which is at about $E_\gamma = 2\text{ MeV}$ the $\sigma_{\text{Coul}ex} = 50\text{ mbarn}$. In this case, the particle- γ events rate is 300 day^{-1} for the first 2_1^+ and 50 day^{-1} for the second 2_2^+ . Since we have a cocktail beam we expect to investigate also neighbor isobars and to obtain for them lifetime information as well. In our case to investigate the nuclei of interest we need three different beams. For the investigation of the reference nucleus ^{84}Kr we need 1 day of beam time, for ^{88}Kr , ^{90}Sr , and ^{86}Se three days, each. We, thus, request 10 days of beam time in total.

References

- [1] A. Arima, T. Otsuka, F. Iachello, I. Talmi, Phys. Lett. B 66 (1977) 205.
- [2] D. Bohle et al., Phys. Lett. B 137, (1984) 27.
- [3] A. Richter, Prog. Part. Nucl. Phys. 34, (1995) 261.
- [4] F. Iachello, Nucl. Phys. A 358, (1981) 89c.
- [5] N. Pietralla et al., Phys. Rev. Lett. 83, (1999) 1303.
- [6] N. Pietralla et al., Phys. Rev. Lett. 84, (2000) 3775.
- [7] C. Fransen et al., Phys. Lett. B 508, (2001) 219.
- [8] N. Pietralla et al., Phys. Rev. C 64, (2001) 031301(R).
- [9] H. Klein et. al., Phys. Rev. C 65, (2002) 044315.
- [10] V. Werner et. al., unpublished.
- [11] A. Lisetskiy et al., Nucl. Phys. A 677, (2000) 100.
- [12] G. A. Lalazissis, M. M. Sharma, Nucl. Phys. A 586 (1995) 201.
- [13] J.K. Tuli, Nucl. Data Sheets 81, (1997) 331.
- [14] T. Rzaca-Urban et al., Eur. Phys. J. A 9, (2000) 165.
- [15] Balraj Singh, Nucl. Data Sheets 94, (2001) 1.
- [16] E. Fermi, Z. Phys. 29, (1924) 315.
- [17] K. Adler et al., Rev. Mod. Phys. 28, (1956) 432.

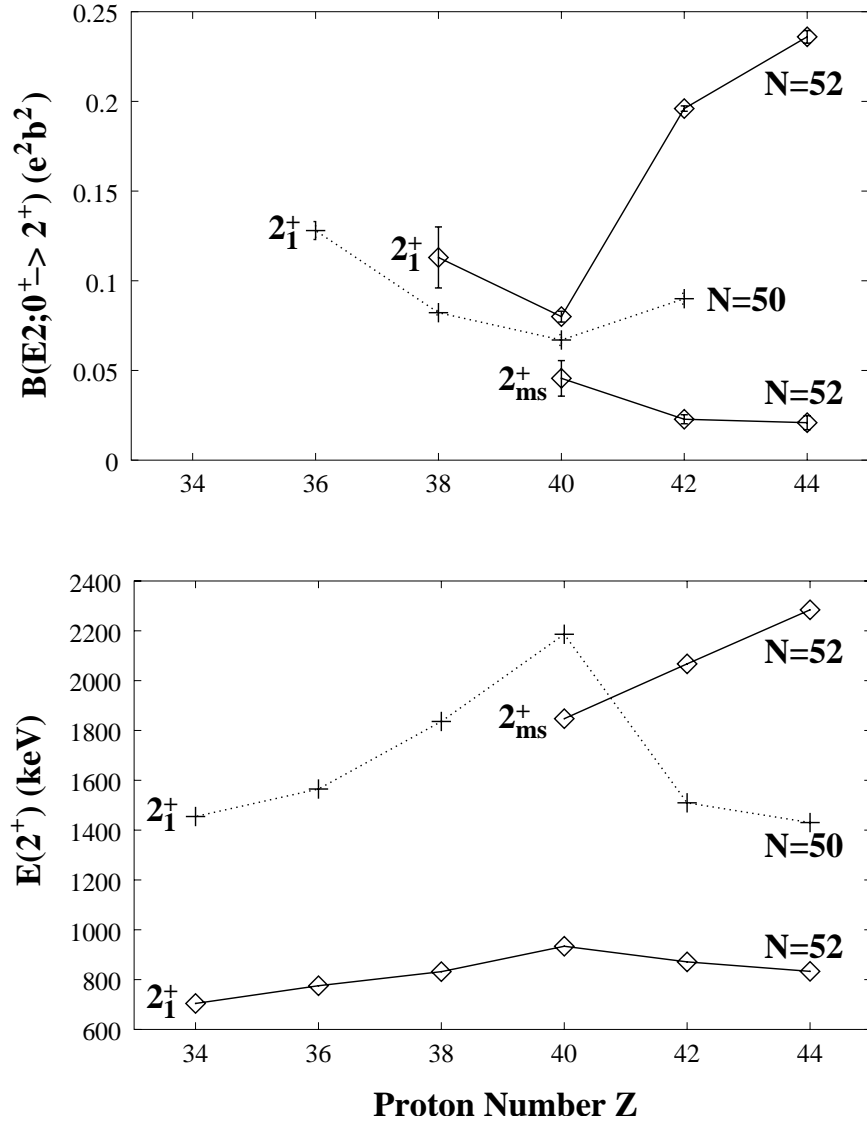


Figure 1: Experimental data on 2^+ states in $N = 50$ and $N = 52$ isotones. The available $B(E2; 0_1^+ \rightarrow 2_1^+, 2_{ms}^+)$ transition strengths are shown at the top. The energy of the corresponding 2^+ levels is shown in the bottom panel.

Relativistic Coulomb excitation of nuclei near ^{100}Sn

A RISING proposal

C. Fahlander, J. Ekman, M. Mineva, D. Rudolph, et al.

Department of Physics, Lund University

M. Górska, H. Grawe, A. Blazhev, et al.

GSI, Darmstadt, Germany

J. Nyberg, et al.

Department of Radiation Sciences, Uppsala University, Sweden

B. Cederwall, et al.

Royal Institute of Technology, Stockholm, Sweden

M. Benteley

Department of Physics, Keele University, UK

G. de Angelis, A. Gadea, et al.

. Laboratori Nazionali di Legnaro, Padova, Italy

M. Palacz, et al.

Heavy Ion Laboratory, Warsaw University, Poland

D. Sohler, et al.

Institute for Nuclear Research, Debrecen, Hungary

P. Nolan et al.

Liverpool University, Liverpool, UK

1 Physics motivation

^{100}Sn is the heaviest isospin symmetric doubly-magic nucleus, which is particle bound. This gives rise to a lot of interesting physics, which we can hope to study in ^{100}Sn and in nuclei in its vicinity. One of the burning questions in nuclear structure physics is whether the shell closures as we know them today are valid also at the limits of stability. This question is related to the E2 polarizability and shape response of the magic core, which we could get information on in ^{100}Sn if we have measured the energy of its first excited 2^+ state, and the transition rate from that state to the ground state. However, although ^{100}Sn was observed a few years ago in relativistic projectile fragmentation reactions, both at GSI and at GANIL, it will not be possible to study its detailed structure before we have available radioactive beams from the next generation

of RNB facilities, but meanwhile we can learn about E2 correlations of the ^{100}Sn core by studying nuclei close to it.

In the past we have done many experiments involving heavy-ion fusion evaporation reactions in conjunction with large gamma-ray detector systems in a very successful collaboration between many universities and laboratories in Europe. The partial level structures have been measured in the light Sn isotopes, the lightest being ^{102}Sn , which together with ^{98}Cd are the closest neighbours to ^{100}Sn with known excited states. In particular it has been possible to measure the lifetimes of low-lying isomeric 6^+ states in the even Sn isotopes [1, 2], and of an isomeric 8^+ state in ^{98}Cd [3]. These measurements were followed by an enhanced interest from the experimental as well as from the theoretical side [4, 5, 6, 7]. The lifetimes range from a few ns to some few hundred ns, which give the $B(E2)$ values of the 6^+ to 4^+ and 8^+ to 6^+ transitions in the order of a few W.u. The $B(E2)$ values provide information on the neutron and proton effective charges, which are measures of the E2 polarizability (n-particle,n-hole excitation) of the core [6, 8]. They can be adjusted in, e.g., shell model calculations to reproduce the measured $B(E2)$ values. However, the $B(E2)$ values are sensitive also to effects other than core polarization, e.g., to the single particle energies of the orbits involved in the transitions, so care has to be taken not to draw too far reaching conclusions. The single particle level energies lack the experimental values especially for low spin orbitals, which however may contribute significantly to the strength of the $6^+ \rightarrow 4^+$ transition for even Sn isotopes [9]. The $B(E2;2^+ \rightarrow 0^+)$ values are however the most sensitive test of E2 correlations related to core polarization.

Figure 1 shows the two particle separation energy differences, the measured $B(E2;2^+ \rightarrow 0^+)$ values and the excitation energies of the 2^+ states for the light $Z=50$ Sn isotopes and $N=50$ isotones [10]. The level energies of the 2^+ states in the Sn isotopes above ^{102}Sn are known experimentally and their almost constant values along the whole chain is the classical example for the generalized seniority scheme [11, 12]. This indicates that the 2^+ states may be described as one broken pair upon a ground state condensate of 0^+ pairs. The transition probabilities known only for stable Sn isotopes show an irregular behaviour as they are the most sensitive to the details of the shell structure and to quadrupole collective effects. The aim of the present proposal is therefore to measure the $B(E2;2^+ \rightarrow 0^+)$ values for the missing nuclei using relativistic Coulomb excitation. Their measurement, by standard Doppler methods, is hampered by the existence of the higher lying isomeric states, and they are too fast for electronic lifetime measurements. Therefore, Coulomb excitation is the only way to obtain this very important piece of structure information.

The nuclei of interest are the $Z=50$ tin isotopes ^{102}Sn , ^{104}Sn , ^{106}Sn , ^{108}Sn , and ^{110}Sn , and the $N=50$ isotones ^{94}Ru , ^{96}Pd , and ^{98}Cd . The Coulomb excitation of odd mass

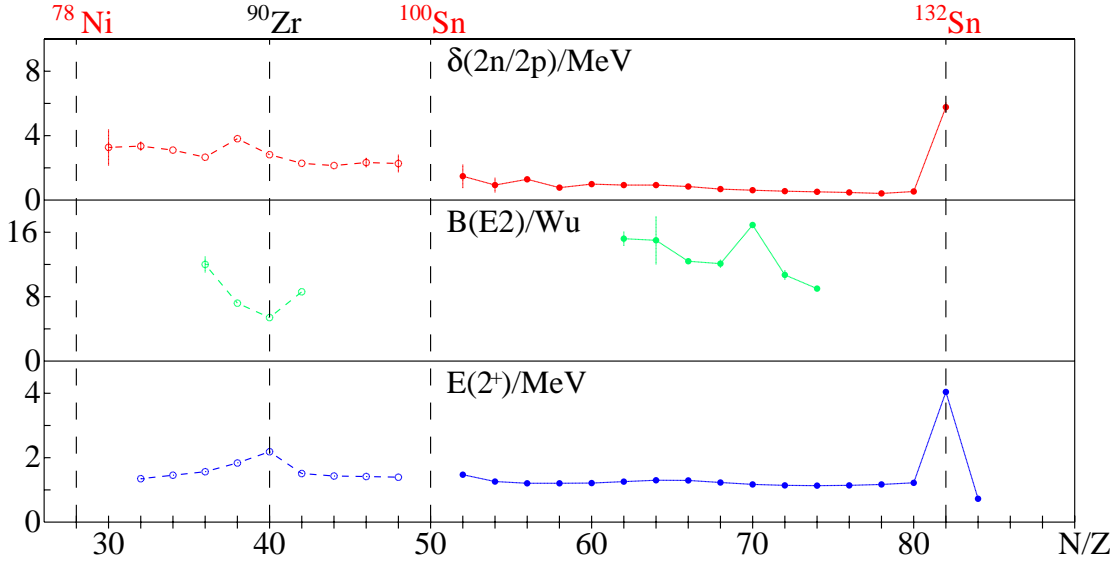


Figure 1: Excitation energies of the 2^+ states, the E2 strength $B(E2:2^+ \rightarrow 0^+)$ and the second difference of the ground state binding energies δ_{2n} resp. δ_{2p} for the Sn isotopes from $N=50$ to $A=84$ (solid line) and the $N=50$ isotones from $Z=32$ to $Z=48$ (dashed line), the isospin mirrors to the $N \leq Z$ Sn isotopes [10].

Sn isotopes, which are produced simultaneously could give the first information on the single particle energy of the $3s_{1/2}$ orbital. The large matrix element of the stretched E2 transition between $2d_{5/2}$ and the $3s_{1/2}$ strongly favours Coulomb excitation in the search for this quantity. In in-beam fusion-evaporation or β -decay experiments those states are not populated. In some cases of the even Sn isotopes, where the lifetime of the isomer is long enough to survive the passage through the FRS, it will be possible to Coulomb excite the nucleus from its isomeric state, and measure the $B(E2)$ value to the first excited state above the isomer. Also we would like to measure ^{112}Sn and ^{92}Mo , where the $B(E2;2^+ \rightarrow 0^+)$ values are known, because they would provide very good calibration points.

2 Count rates

We propose to produce the isotopes by means of projectile fragmentation reactions at around 750 MeV/u primary beam energy. The reaction products will be slowed down by degraders to about 100 MeV/u, and Coulomb excited by a secondary target, either from their ground states or from their isomeric states. The reaction products will be traced from the primary target to the secondary target placed at the focal plane S4 of the FRS. The scattered reaction products will be detected and identified by means of

A and Z, and the gamma rays following the Coulomb excitation will be measured in RISING.

The number of secondary beam particles at S4, N_{S4} , is given by the production cross section times the luminosity times the transmission through the FRS: $N_{S4} = \sigma \cdot L \cdot T_{FRS}$. Assuming a primary beam intensity of 10^9 particles per second, and a primary target of 1.6 g/cm^2 ^9Be , the luminosity L is $10^{32} \text{ cm}^{-2}\text{s}^{-1}$ (a 1.3 g/cm^2 ^{208}Pb target gives a factor of 25 smaller luminosity). A production cross section of 10^{-5} barn thus gives 300 secondary particles per second at S4 assuming that the transmission through the FRS is 30%.

The number of excitations to the 2^+ state is: $N_{2^+} = N_{S4} \cdot \sigma_{2^+} \cdot 4 \cdot 10^{20}$, where σ_{2^+} is the Coulomb excitation cross section of the 2^+ state and $4 \cdot 10^{20}$ is the number of atoms in the secondary target assuming it to be ^{208}Pb with a thickness of 200 mg/cm^2 . This gives about 6000 excitations to the 2^+ state per day with a Coulomb excitation cross section of 400 mb.

The number of detected γ rays is: $N_\gamma = N_{2^+} \cdot \epsilon_\gamma$, where ϵ_γ is the photo peak efficiency of RISING. Assuming it to be 2% (for Doppler shifted γ -ray of 1.2 MeV) this gives 120 detected γ decays per day in the photo peak. For the experiment to be feasible it will be necessary to detect about 50 γ decays per day, which then sets the limit of the production cross section to be larger than about $4 \cdot 10^{-6}$ barn.

The production cross sections for the isotopes of interest are estimated using the EPAX code and shown in Table 1 for different primary beam and target combinations, namely for a ^{112}Sn , a ^{124}Xe , and a ^{129}Xe beam, all on a ^9Be target. Using the limit above on the production cross section we would thus be able to study the tin isotopes down to ^{104}Sn using the ^{124}Xe beam, as well as ^{94}Ru and ^{96}Pd . Unfortunately, ^{98}Cd and ^{102}Sn seem to be out of reach. However, the experimental cross sections for the ^{112}Sn beam [13], also shown in the table, are in almost all cases larger than the EPAX estimates, in some cases even an order of magnitude larger, e.g., for ^{104}Sn .

Calculations using the MOCADI code supports the estimated count rates above. We thus ask for 18 shifts (6 days) of beam time using ^{124}Xe as a primary beam. This includes 3 days for ^{104}Sn which will give about 200 counts in the photo peak of the $2^+ \rightarrow 0^+$ transition, and an average of 1 shift per each other case mentioned in Table 1, 2 shifts for calibration runs ^{112}Sn and ^{92}Mo , and 2 shifts for changing of the FRS settings.

References

- [1] R. Schubart *et al.*, Z. Phys. A 352 (1995) 373.
- [2] M. Lipoglavšek *et al.*, Phys.Lett. B440 (1998) 246.
- [3] M.Górska *et al.*, Phys.Rev.Lett. 79 (1997) 2415.
- [4] C. Fahlander *et al.*, Phys. Rev. C63 (2001) 021307(R).
- [5] A. Covello *et al.*, Proc. 6th Int. Spring Seminar on Nuclear Physics - "Highlights of modern nuclear structure", ed. A. Covello, World Scientific, Singapore, 1999, p.129.
- [6] F. Nowacki, Proc. SM2K, Nucl. Phys. A, in print.
- [7] T. Engeland, *et al.*, Phys. Rev. C61 (2000) 021302(R)
- [8] H. Grawe *et al.*, AIP Conf. Proc., TOURS Symp. Nucl. Phys. IV, Tours, France, 2000, p. 287
- [9] M.Górska *et al.*, Phys.Rev. C 58 (1998) 108.
- [10] H. Grawe, M. Lewitowicz, Nucl. Phys. A693 (2001) 116.
- [11] I. Talmi, Nucl. Phys. A 172 (1971) 1.
- [12] N. Sandulescu, *et al.*, Phys. Rev. C55 (1997) 2708.
- [13] A. Stolz, Ph. D. thesis, T.U. München, 2001.

Table 1: EPAX-2 and experimental cross sections in barns

| Isotope | EPAX-2 $^{112}\text{Sn}-^9\text{Be}$ | Experiment $^{112}\text{Sn}-^9\text{Be}$ | EPAX-2 $^{124}\text{Xe}-^9\text{Be}$ | EPAX-2 $^{129}\text{Xe}-^9\text{Be}$ |
|-------------------|---|---|---|---|
| ^{110}Sn | 2.2-02 | – | 1.13-02 | 6.9-03 |
| ^{108}Sn | 1.1-03 | 4.1(1.7)-03 | 3.7-03 | 1.4-03 |
| ^{106}Sn | 2.5-05 | 1.4(8)-04 | 3.2-04 | 7.3-04 |
| ^{104}Sn | 3.0-07 | 2.1(9)-06 | 5.6-06 | 6.9-07 |
| ^{103}Sn | 2.4-08 | 1.7(8)-07 | 3.6-07 | 3.3-08 |
| ^{102}Sn | 1.5-09 | 7.0(2.6)-09 | 1.4-08 | 9.5-10 |
| ^{101}Sn | 9.8-11 | 2.1(9)-10 | 3.1-10 | 1.7-11 |
| ^{98}Cd | 1.6-07 | 1.0(4)-07 | 7.3-08 | 8.7-09 |
| ^{96}Pd | 1.8-04 | – | 6.4-05 | 1.7-05 |
| ^{94}Ru | 5.9-03 | – | 2.9-03 | 1.5-03 |

Nuclear magicity at $Z\sim 50$ $N\sim 82$ investigated through knock-out reaction of ^{132}Sn

G. de Angelis, M. Axiotis, A. Gadea, N. Marginean, T. Martinez, D.R. Napoli
INFN, Laboratori Nazionali di Legnaro, Legnaro, Italy

E. Farnea, S. Lenzi, S. Lunardi, R. Menegazzo, C. Ur
INFN, Padova, Italy

W. Gelletly, Z. Podolyák
Department of Physics, University of Surrey, Guildford, UK

B. Rubio, A. Algora, E. Nacher, L. Caballero
Instituto de Fisica Corpuscular, Valencia, Spain

A. Bonaccorso
INFN, Sezione di Pisa

N. Blasi, A. Bracco, F. Camera, B. Million, S. Leoni
INFN, Sezione di Milano

C. Petrache, G. Lo Bianco
Dipartimento di Matematica e Fisica, Università di Camerino, Camerino, Italy

H. Grawe, M. Gorska...?
GSI

Abstract:

The availability of radioactive nuclear beams of good intensity and optical quality makes possible the use of direct nuclear reactions to investigate fundamental properties such as the nuclear matter distribution, deformation and the evolution of shell structure very far from stability. The predicted reduction in the spin-orbit term in the nuclear force with increasing neutron excess is attracting considerable interest because it underlies major changes in the single particle energies of intruder states and shell quenching effects .

A recent study of the structure of the very neutron-rich Sn and Sb nuclei using a resonance ionization laser ion source at CERN/ISOLDE has given indication of a possible signature of the effects of a more harmonic-oscillator-like potential .

Here we propose to investigate at RISING the magicity of the $Z=50$, $N=82$ shell by means of knock-out reactions using a beam of ^{132}Sn secondary fission fragments produced at the FRS and detecting the gamma rays de-exciting the states in ^{131}Sn .

We request five days of beam time at the FRS in order to be able to extend the spectroscopic information of the region and determine spectroscopic factors.

Motivation:

Neutron-rich nuclei close to the $N=20$ and 28 shell gaps have attracted particular interest because of the possible existence of anomalies in the shell structure. It has been suggested on the basis of self consistent mean field calculations that the major $N=28$ shell gap disappears when approaching $Z=16$ and the energy surfaces become very soft, with close lying and shallow minima corresponding to different deformations [1,2,3]. There is also evidence of the shrinking of the shell gaps from the results of astrophysical calculations of the nuclear abundances of heavy elements, created in the rapid neutron-capture process of nucleosynthesis. The predictions of the disappearance of the "classical" shell gaps have been further reinforced by Hartree-Fock-Bogoliubov calculations with the SKP force [4,5] and by mass predictions from the infinite nuclear matter model [6]. Experimentally the weakening of the neutron shell structure near the drip line has been investigated for both $N=20$ and $N=28$ nuclei [7,8]. Evidence for such an effect at $N=50$ has also been put forward by Kratz et al. [9,10] for the decay of the r -process waiting-point isotope ^{80}Zn . A recent study of the structure of the very neutron-rich Sn and Sb nuclei using a resonance ionization laser ion source at CERN/ISOLDE has given indication of a possible signature of the effects of a more harmonic-oscillator-like potential [11].

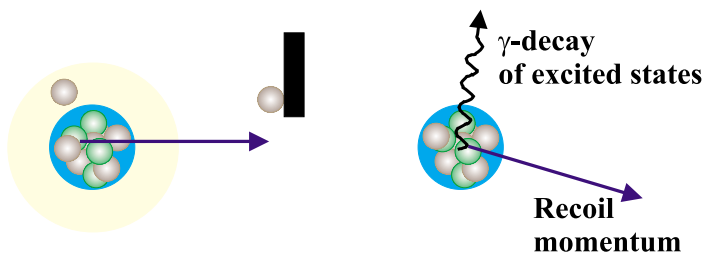


Figure 1: Pictorial view of Knock Out Reactions. Spectroscopic factors are deduced from the intensities of gamma rays depopulating the excited states in the $A-1$ fragment. The l -value of the ejected nucleon can be determined from the momentum distribution of the particle.

To investigate this phenomenon it is straightforward to follow specific nuclear properties along extended isotopic chains, from stable nuclei towards the limit of nuclear stability. A variety of different nuclear reaction mechanisms has been used for the investigation of nuclei far from stability, such as Coulomb excitation [12], elastic and inelastic scattering [2], transfer [13] and knock-out reactions [14]. Coulomb excitation and proton scattering experiments have been used to probe the proton and neutron densities respectively, but the limitations on secondary beam intensities have precluded the extension of such studies above the $N=28$ shell closure.

Direct evidence of the breakdown of the $N=8$ shell closure has recently been obtained through the measurement of the partial cross sections and corresponding momentum distributions in the one-neutron knockout reaction (^{12}Be , $^{11}\text{Be} + \gamma$) on a ^9Be target at 78 MeV/nucleon [14]. The resulting spectroscopic factors have shown wave functions with substantial contributions from intruder states. Again similar studies for other shells have been limited until now by the low production rates of beams of unstable nuclei.

Here we propose to investigate the magicity of the $Z=50$, $N=82$ shell using a beam of ^{132}Sn produced by secondary fission fragments at the FRS.

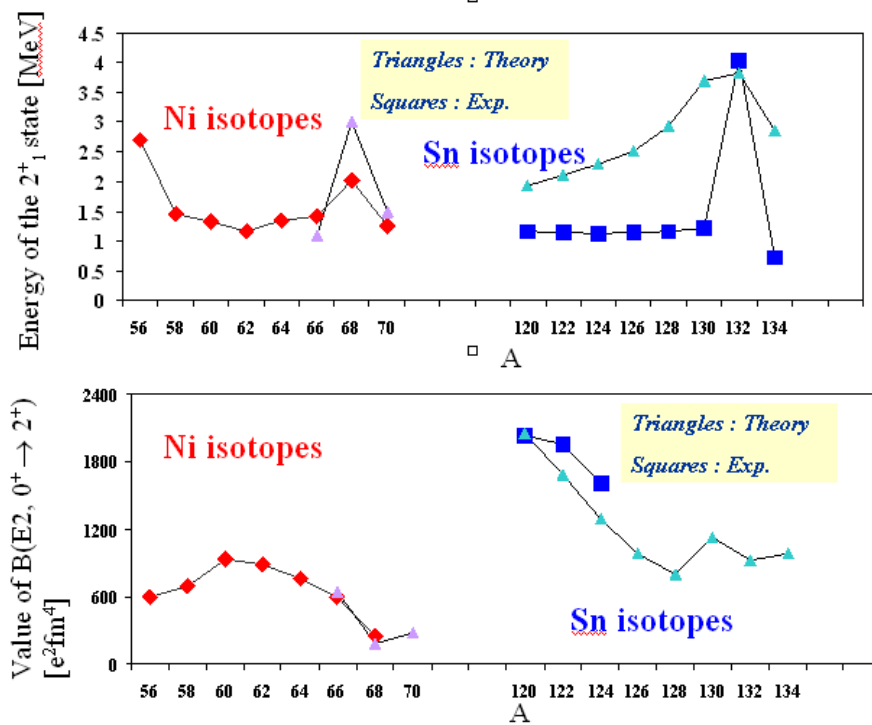


Figure 2: Comparison between the theoretical and experimental values of the energies and $B(E2)$ s associated with the lowest 2^+ states in even Ni and Sn isotopes. The data are from reference 15 and the theory from 16.

In fig.2 the energy systematics of the low-lying 2^+ states is reported for a number of isotopes of Ni with $28 \leq N \leq 40$ and for Sn isotopes with $70 \leq N \leq 84$ (cf. Fig. 2). The high value observed for $^{132}_{50}\text{Sn}_{82}$ fits well with its doubly magic character. Still missing, however are measurements of the reduced transition probabilities and studies of more neutron rich isotopes, as well as the properties of negative parity states including octupole vibrations. Recently the $B(E2)$ value for ^{68}Ni has been measured at Ganil [17]. The unexpected small value, together with the small two-neutron separation energy, has been interpreted in terms of an erosion of the $N=40$ harmonic-oscillator subshell by neutron-pair scattering.

While calculations with different forces predict rather similar excitation energies for low-lying collective surface vibrations, they predict reduced transition probabilities which differ by factors of two. This reflects the limitations in our understanding of effective nuclear forces which can only be overcome with data on unstable nuclei.

Spectroscopic factors in ^{132}Sn :

The $N=82$ shell closure in unstable nuclei has only been partially investigated. The determination of the spectroscopic factors in $A-1$ nucleus (for states populated in knock-out reactions by detecting the gamma ray de-exciting the states) will provide detailed information on the mixing of single particle states with more complicated configurations. The mixing is expected to occur mainly with configurations containing a low-lying surface vibrational mode. Estimates of absolute one-particle removal cross sections for knock out reactions indicate cross sections of the order of a few mb/sr —fig.4-

In addition the evolution of the single-particle levels, of which only a few are known, could be studied with knock out reactions by detecting the gamma rays deexciting the states in nuclei around the $Z=50$ proton closed shell and the $N=82$ neutron shell. Naively the single-particle gap and the 2^+ excitation energy ($\approx 5 \text{ MeV}$ and $\approx 4 \text{ MeV}$, respectively) remind us the

situation for ^{208}Pb (≈ 4 MeV for both quantities), where the pairing correlation energy (pairing gap) associated with the systems with two neutrons outside a closed shell (i.e. ^{134}Sn and ^{210}Pb) is approximately 0.7 and 1.4 MeV respectively.

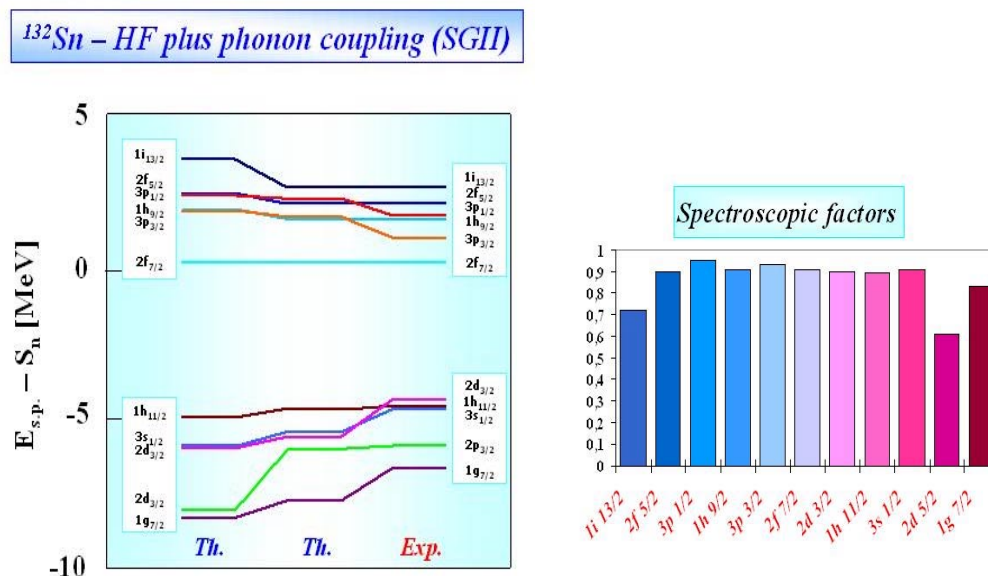


Figure 3: **Left panel** : Single-particle and single-hole levels of $^{132}\text{Sn}_{50}$. The experimental values (on the right, from reference 15) are compared with two predictions (from reference 16). Those on the left are based on Hartree-Fock (HF) calculations with the SGII effective interaction while the one shown in the middle also includes the self energy contributions from the coupling to collective phonons. **Right panel** : Spectroscopic factors associated with the different single particle (and hole) levels obtained in the HF plus phonon coupling.

Figure 3 shows spectroscopic factors for ^{132}Sn obtained through Hartree-Fock calculations with SGII effective interaction (right), and including (middle) the coupling to collective phonons. The values close to unity underline the doubly magic character of the ^{132}Sn .

A clearly related topic is the study of the spin-orbit splitting in the ^{132}Sn nucleus i.e. the $vd_{5/2} - vd_{3/2}$ and the $\pi g_{7/2} - \pi g_{9/2}$ splittings. The spin-orbit splitting plays an important role in determining the binding and structure of nuclei. Indeed, the introduction of spin-orbit splitting of the nucleon orbitals in the nuclear mean-field potential was the key to the development of the nuclear shell model. Depending on the relative orientation of the spin and the orbital angular momentum, the energy of the associated nuclear state is pushed up or down. This effect is essential for the understanding of the magic numbers. According to certain model predictions, the energy splitting of these spin-orbit partners should decrease or even vanish far from stability for very neutron-rich isotopes.

A direct way to measure the ground state structure of ^{132}Sn is to determine the spectroscopic factors for the removal of a neutron. Already the observation of the decay of the $7/2^-$ level in the gamma spectrum of ^{131}Sn should directly probe the occupancy of the $2f_{7/2}$ orbit. Here for example the neutron closed shell configuration $(h_{11/2})^{12}$ would give spectroscopic factors of $12/(2j+1)$ for the $11/2^-$ and 0 for the $7/2^-$ states. Also the

experimental determination of the single particle character of the $5/2^+$ state at 1.655 MeV above the $vd_{3/2}$ ground state, should shed some light on the relatively low value of the $vd_{5/2}$ - $vd_{3/2}$ spin orbit splitting.

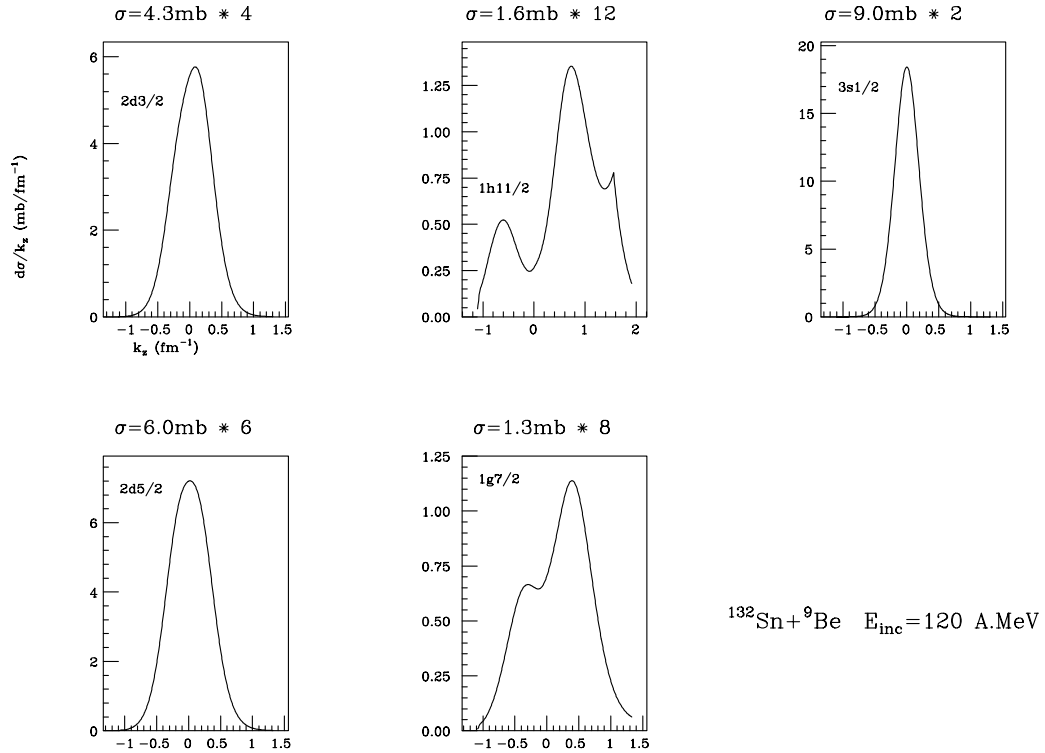


Figure 4 : Knock out cross sections calculated for the $^{132}\text{Sn} + ^9\text{Be}$ reaction at 120 MeV. The binding energies are taken from ref.15. These estimate do not change very much for energies up to 300 MeV.

Experimental details:

The experiment involves the measurement of the partial cross sections for the population of the final states of the residues formed in the one nucleon knockout reaction $^9\text{Be}(^{132}\text{Sn}, ^{131}\text{Sn} + \gamma)^9\text{Be}$. The secondary beam will be produced by induced fission of an ^{238}U beam and analysed in mass and momentum by the FRS.

The expected production rate of ^{132}Sn at the secondary target position is of $\sim 5 \cdot 10^2$ atoms/s with a momentum spread of 1%.

The fission fragments will be analysed in charge and mass by a standard FRS detectors. The recoils from the secondary target will be identified in the CATE telescope.

The ^{132}Sn beam will be incident on a 1000 mg/cm^2 ^9Be target. Assuming a cross section of $\sim 100 \text{ mb}$ the estimated production of ^{131}Sn is of 3.8 atoms/s. The high granularity of the RISING germanium array should allow us to achieve a gamma resolution of 18 keV at 1.3 MeV. Assuming a gamma efficiency for Rising of 2% (including the Lorentz boost) we expect a counting rate in the Ge detectors of $\sim 6 \cdot 10^3$ in 24 h.

With the calculated rates and assuming the cross sections reported in fig.4, we request five days of beam time at the FRS in order to be able to determine spectroscopic factors with a

precision better than 10%. A similar investigation in the Ni region could be based on the data of the proposal (this PAC) of A. Bracco.

References :

- [1] E. Khan et al. ; *Nucl. Phys. A* 694 (2001) 103
- [2] F. Marechal et al. ; *Phys. Rev. C* 60 (1999) 034615
- [3] H. Scheit et al. ; *Phys. Rev. C* 63 (2000) 014604
- [4] J. Dobaczewski et al. ; *Phys. Rev. Lett.* 72 (1994) 981
- [5] J. Dobaczewski et al.; *Phys. Scr.* T56 (1995) 72
- [6] R.C. Nayak *Phys. Rev. C* 60 (1999) 064305
- [7] N.A. Orr et al.; *Phys. Lett. B* 258(1991) 29
- [8] O. Sorlin et al.; *Phys. Rev. C* 47 (1997) 2941
- [9] K.L. Kratz et al.; *Phys. Rev. C* 38 (1998) 278
- [10] B. Pfeiffer et al. ; *Z. Phys. A* 357 (1997) 235
- [11] J. Shergur et al. ; *Nucl. Phys. A* 682 (2001) 493c
- [12] T. Glasmacher, *Annu. Rev. Nucl. Part. Sci.* 48 (1998) 1
- [13] S. Fortier et al. ; *Phys. Lett. B* 461 (1999) 22
- [14] A. Navin et al. ; *Phys. Rev. Lett.* 85 (2000) 266
- [15] H. Grawe and M. Lewitowicz, *Nucl. Phys. A* 693 (2001) 116
- [16] F. Barranco and G. Colo', *private comm.*
- [17] O. Sorlin et al.; *Phys. Rev. Lett.* 88 (2002) 092501

Coulomb Excitation at Intermediate Energies - Angular Distribution and Particle- γ Angular Correlation Measurement -

A. Maj, M. Kmiecik, W. Meczynski, J. Styczen
The Henryk Niewodniczanski Institute of Nuclear Physics,
31-342 Krakow, ul. Radzikowskiego 152, Poland

E. Lubkiewicz
Physics Institute, Jagellonian University, Reymonta 4, 30-059 Cracow, Poland

A. Bracco, F. Camera, B. Million, S. Leoni
Milano University and INFN, Milano, Italy

H.J. Wollersheim and the Rising collaboration
Gesellschaft für Schwerionenforschung, P.O. Box 110552, D-64291 Darmstadt, Germany

Coulomb excitation is a well-established experimental probe in nuclear physics, which is sensitive to the internal structure of the nuclei involved. Traditionally, stable targets are bombarded with stable heavy-ion beams at energies well below the Coulomb barrier between the projectile and the target. With the recent availability of short-lived beams of β -unstable nuclei it has become desirable to apply the same electromagnetic probe to exotic nuclei, which cannot be prepared into targets. This task is somewhat complicated by the properties of the radioactive beams; they are generally several orders of magnitude less intense than stable beams, and the beams prepared by in-flight separation have energies of e.g. $T_{lab}/A_1=100$ MeV/nucleon ($v/c\approx 0.43$). Intermediate-energy Coulomb excitation takes advantage of these large exotic beam velocities and compensates for the low exotic beam intensities by employing very thick secondary targets ($500\text{mg}/\text{cm}^2$).

1. Angular distribution measurement

To use the theory of electromagnetic interactions [1,2] to relate the measured excitation cross sections to electromagnetic matrix elements, the experimentalist must assure that nuclear contributions to the excitation process are small. This can be accomplished by keeping the projectile and target nuclei at a safe distance from each other so that the short-range nuclear force does not contribute. This is accomplished in experiments at intermediate beam energies by selecting reactions with an extremely forward scattering angle θ_{lab} , corresponding to a large impact parameter b or distance of closest approach $R\approx b$. With the relativistic expression for the deflection function one obtains

$$\theta_{lab} [rad] = \frac{2.88 * Z_1 * Z_2 * [931.5 + (T_{lab} / A_1)] * 1}{A_1 * [(T_{lab} / A_1)^2 + 1863 * (T_{lab} / A_1)] * b},$$

where Z_1 and Z_2 denote the nuclear charge of the collision partners, A_1 the projectile mass, T_{lab} the laboratory beam energy in MeV and b the impact parameter in fm.

One aim of the present proposal is a measurement of an angular distribution, in order to check the validity of the semi classical Coulomb excitation approach. For impact parameters around grazing incidence, electromagnetic cross sections are reduced due to nuclear reactions absorbing part of the flux. Most frequently, the electromagnetic cross sections are computed adopting a minimum impact parameter b_{min} below which electromagnetic excitation is cutoff. An appropriate choice of b_{min} is crucial in calculating reliable Coulomb excitation cross sections. Several empirical parameterizations (e.g. [3]) for the nuclear interaction radius $R_{int}\approx b_{min}$ exist, which are based on low-energy reaction data. For projectile-target combinations like ^{86}Kr on ^{197}Au or ^{136}Xe on ^{197}Au one obtains an interaction radius of $R_{int}=14.2\text{fm}$ (15.0fm) resulting in a grazing angle of $\theta_{max}=35\text{mrad}$ (32mrad) at a bombarding energy of 100 MeV/nucleon.

Measurements of angle-differential cross sections are often washed out in relatively thick targets, as usually applied, by multiple scattering to small angles (angular straggling). Therefore, we propose to use rather thin ($50\text{mg}/\text{cm}^2$) Au targets, which lead to a small angular straggling of 2.7mrad . The use of a stable Kr beam has the advantage not to be limited in beam intensity and requires no particle identification before the Coulomb excitation target. The obtained result on the minimum impact

parameter b_{min} is essential for all other planned Coulomb excitation experiments using radioactive projectiles. It will be used together with a mass identification to calculate b_{min} and to extract electromagnetic matrix elements $B(E\lambda)$ from the measured Coulomb excitation cross sections.

2. Particle- γ angular correlation measurement

Measuring the Coulomb excitation cross section by counting deexcitation γ -rays requires also a precise knowledge of the particle- γ angular correlation. The angular correlation of the photons measured in the laboratory is a convolution of the intrinsic angular distribution of the photons in the projectile frame and the Lorentz boost from the projectile frame into the laboratory frame. This is depicted in Fig.1 for an E2-decay from a 2^+ state to the 0^+ ground state in ^{20}Ne , which was excited in a Coulomb excitation experiment on a ^{208}Pb target at a bombarding energy of 200 MeV/nucleon. The population of magnetic sub states in the excited state depends on the multipolarity λ of the transition, the spin of the state and the minimum impact parameter b_{min} . If the excitation mechanism is purely Coulomb and if the spin of the excited state is known, then the particle- γ angular correlation can be calculated for a given multipolarity by integration over the impact parameter from $b=b_{min}$ to $b=\infty$.

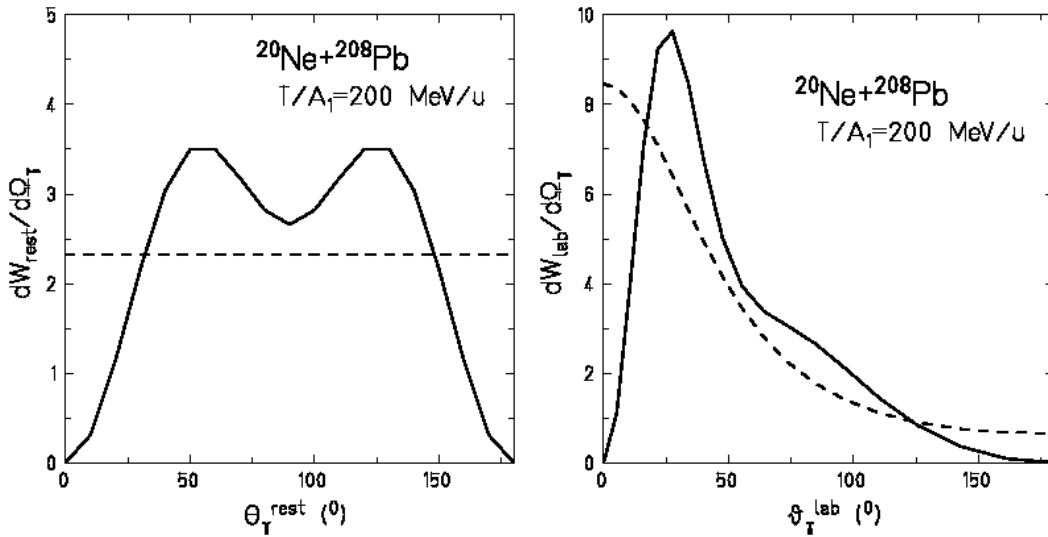


Fig.1: Particle- γ angular correlation for a $2^+ \rightarrow 0^+$ E2-transition in ^{20}Ne (solid line) calculated in the projectile rest frame (left) and in the laboratory frame (right). The ^{20}Ne projectile was excited on a ^{208}Pb target at a bombarding energy of 200 MeV/nucleon. Dashed line – isotropic distribution in the projectile rest frame.

As one can see from Fig.1, the pronounced double-humped E2-angular correlation (projectile frame) can hardly be distinguished from an isotropic distribution (dashed line) in the laboratory frame.

However, for a symmetric γ -setup - Ge-detectors on the left hand side ($\Phi_\gamma=0^0$) and on the right hand side ($\Phi_\gamma=180^0$) of the beam direction – an intensity ratio can be determined which is sensitive to the particle- γ angular correlation if plotted as a function of the azimuthal projectile angle Φ_p (see Fig.2). The transformation from the projectile rest frame into the laboratory frame is the same for Ge-detectors positioned at the same polar angles (θ_γ) and extreme forward scattering of the projectiles.

The proposed particle- γ angular correlation measurement will be performed for the first time in Coulomb excitation measurements at intermediate energy. The γ -rays deexciting the 2^+ state will be detected in Ge-clusters detectors, while scattered particles in the segmented Si/CsI telescope. It will also allow us to use this correlation for radioactive ion beams to determine the multipolarity λ of γ -transitions, which is crucial for nuclear structure investigations of unknown level schemes. In addition,

we have to determine the maximum slope of the particle- γ angular correlation for nuclear g-factor measurements of short-lived states using the transient magnetic field method.

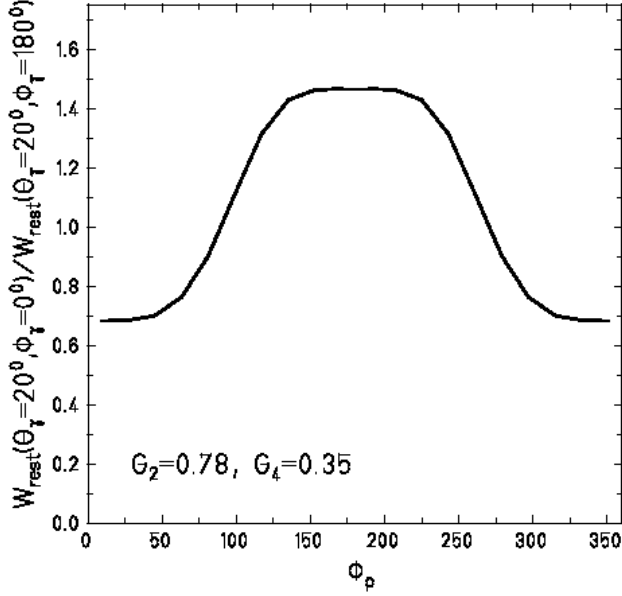


Fig.2: Particle- γ angular correlation for a $2^+ \rightarrow 0^+$ E2-transition in the projectile rest frame as a function of the azimuthal projectile angle Φ_p . G_2 and G_4 are the attenuation coefficients due to hyperfine interactions in vacuum.

3. Beam time request

For the particle- γ angular correlation measurement of ^{132}Xe projectiles excited on a Au or Pb target we estimate a total beam time of 3 days which also includes the determination of the angular distribution. This request is based on a target thickness of $50\text{mg}/\text{cm}^2$, a Coulomb excitation cross section of 500mb , a segmentation of the Si/CsI telescope ($\Delta\Phi_p=18^\circ$), the beam intensity of $10^5\text{-}10^6[\text{s}^{-1}]$ and 3% efficiency of the Ge-cluster detectors for gamma energy of the 668 keV , the $2^+ \rightarrow 0^+$ transition in ^{132}Xe .

References

- [1] A. Winter and K. Alder, Nucl. Phys. **A319**, 518 (1979)
- [2] C.A. Bertulani and G. Baur, Phys. Rep. **163**, 299 (1988)
- [3] W.W. Wilcke et al. Atomic Data and Nucl. Data Tables **25** (1980)

Magnetic moments of Xenon and Tellurium isotopes near doubly-magic ^{132}Sn at relativistic beam energies.

K.-H. Speidel, O. Kenn, J. Leske, S. Schielke

Institut für Strahlen- und Kernphysik, Univ. Bonn, D-53115 Bonn, Germany

J. Gerber

Institut de Recherches Subatomiques, F-67037 Strasbourg, France

P. Maier-Komor

Physik-Dept. Technische Univ. München, D-85748 Garching, Germany

S. K. Mandal, H.-J. Wollersheim for the RISING collaboration

Gesellschaft für Schwerionenforschung, D-64220 Darmstadt, Germany

1 Introduction

Magnetic moments are an indispensable source of information on the microscopic structure of atomic nuclei. It results from the fundamental difference of the spin g factors of protons and neutrons, in *sign* and *magnitude*, $g_S(\pi) = +5.586$ and $g_S(\nu) = -3.826$, which enables to determine the nucleonic components of the wave functions of nuclear states. This behaviour was clearly demonstrated in recent experiments on low-spin states of stable *even-A* neodymium isotopes, for which the well established decrease of $g(2_1^+)$ values with decreasing neutron number, approaching the $N = 82$ shell closure, arises from a strong $f_{7/2}$ neutron component in the wave function [1]. It is a general feature, that nuclei near closed shells, in particular with magic neutron and proton numbers, are characterized by orbital specific single particle components in the wave functions, which changes into collective structures when departing from shell closures. The competition between single particle and collective degrees of freedom is sensitively probed by magnetic moments as well as $E2$ transition rates.

For *ps* lifetimes of nuclear states, there is at present only the technique of transient magnetic fields (TF) which provides the necessary field strengths of several *kTesla*, to observe spin precessions with the method of perturbed γ -angular correlations (PAC). The TF are hyperfine fields of the Fermi contact type, which are experienced in fast moving ions during their passage through ferromagnetic materials [2], among which *Gd* provides the best properties in terms of the polarization of the ions. Its Curie temperature of 298 K, however, requires cooling of the target to liquid nitrogen temperature.

TF are well studied and described by empirical parametrizations [3] at intermediate ion velocities, $v \ll Zv_0$ (in units of the Bohr velocity $v_0 = e^2/\hbar$), whereby the field strength generally increases with velocity reaching a maximum at $v = Zv_0$ for *single-electron* ions with its maximum fraction at the $1s$ electron Bohr velocity. Beyond this velocity the field strength decreases towards zero as the ions become fully stripped (see e.g. [4]). Hence,

the largest TF are accomplished for *H-like* ions implying velocities which correspond to relativistic heavy ions.

For these highly charged ions the TF is parametrized as follows:

$$B_{TF} = p_{1s}(Z, host) \cdot q_{1s}(v, Z, host) \cdot B_{1s}(Z) \quad (1)$$

where p_{1s} is the degree of polarization of the $1s$ electron, q_{1s} the ion fraction with a single $1s$ electron and B_{1s} its Fermi contact field as given by,

$$B_{1s}(Z) = 16.7 \cdot K(Z) \cdot Z^3 \text{ [Tesla]} \quad (2)$$

$K(Z)$ is a relativistic correction [5]; the polarization p_{1s} is proportional to $1/Z$ and $q_{1s} \simeq 0.5$ at the Bohr velocity $v \simeq Zv_0$. Our present knowledge on the Z dependence of p_{1s} refers to light ions only, with *Cr*-ions ($Z=24$) as the heaviest species so far investigated in TF measurements [6].

2 First measurements on radioactive $^{132,134,136}\text{Te}$ isotopes and ^{138}Xe

2.1 Nuclear structure motivation and expectation

In comparison to the stable *even-A* Te isotopes $^{120-130}\text{Te}$, which are collective of vibrational nature with $E(4_1^+)/E(2_1^+) \simeq 2.0$, the structure of the unstable neutron- rich isotopes ^{132}Te , ^{134}Te and ^{136}Te is strongly influenced by the $N = 82$ shell closure and the two protons outside the magic $Z = 50$ shell. This feature becomes evident already from their 2_1^+ excitation energies (Fig. 1a).

It is also determined by their proximity to doubly-magic ^{132}Sn ($Z=50, N=82$) and directly relates to neighbouring isotones ^{134}Xe , ^{136}Xe and ^{138}Xe , respectively (Fig. 1b). For stable ^{134}Xe and ^{136}Xe g factors were recently determined for the 2_1^+ and 4_1^+ states clearly exhibiting single proton excitations with dominant $(\pi 1g_{7/2})$ configuration [7]:

$$\begin{array}{ll} ^{134}\text{Xe} : & g(2_1^+) = +0.354(7) \\ & g(4_1^+) = +0.80(15) \end{array} \quad \begin{array}{ll} ^{136}\text{Xe} : & g(2_1^+) = +0.766(45) \\ & g(4_1^+) = +0.83(14) \end{array}$$

It is the large and positive g factor of both states in ^{136}Xe and of the 4_1^+ state in ^{134}Xe which unambiguously shows the dominant proton nature whereas the smaller $g(2_1^+)$ value in ^{134}Xe implies additional neutron hole configurations mainly in the $h_{11/2}$ orbit (with its negative Schmidt value, $g(\nu h_{11/2}) = -0.348$). This structure is nicely confirmed by shell model calculations which in addition yield small admixtures of configurations of neighbouring single particle orbits.

For the isotones ^{132}Te and ^{134}Te we expect for the first 2^+ states very similar g factors although the number of protons in the $g_{7/2}$ orbit is reduced. For ^{136}Te or its isotope ^{138}Xe , where the $f_{7/2}$ orbit is occupied by neutrons, its 2_1^+ g factor should be smaller than that of neighbouring semi-magic ^{134}Te . Evidence for these expectations can only come from measurements, but such behaviour has been observed for the light *Cr* isotopes, where the $g(2_1^+)$ factor peaks at ^{52}Cr with its $N = 28$ shell closure [8].

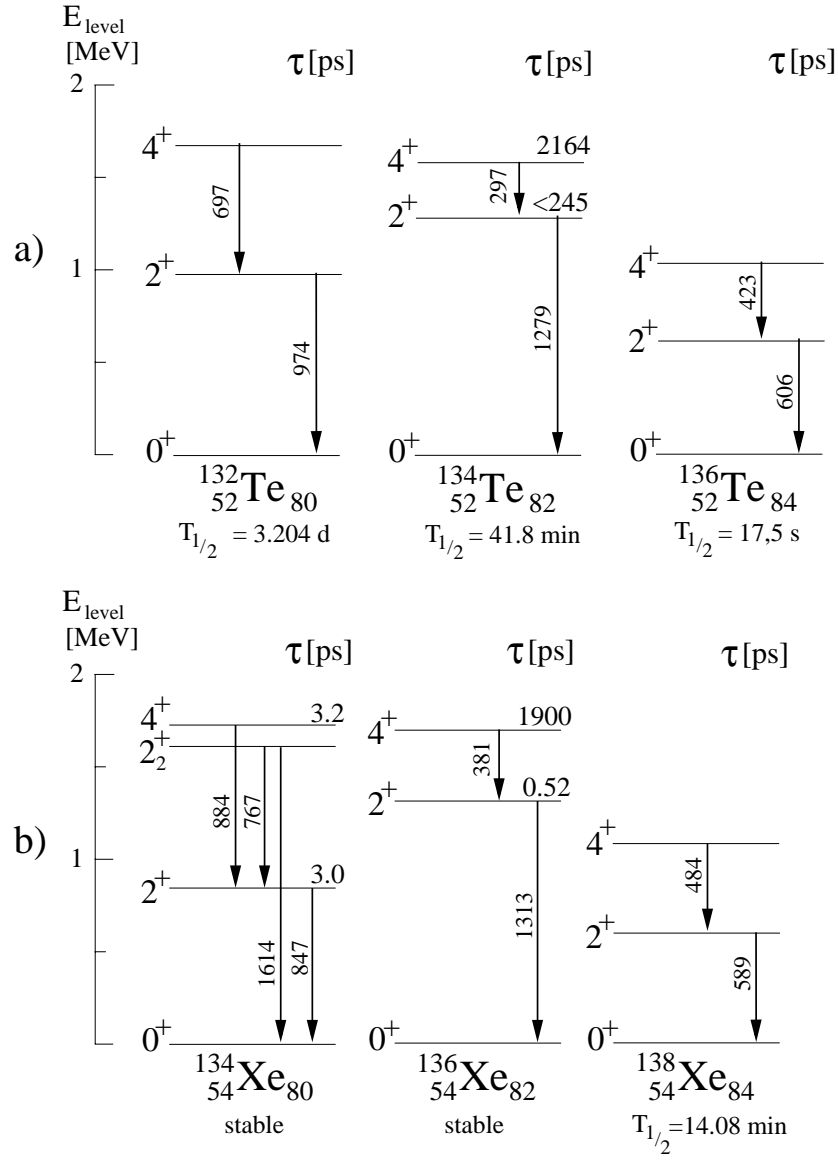


Figure 1: *Low-lying states with relevant γ transitions of even- A (a) unstable Te isotopes and (b) corresponding Xe isotopes.*

2.2 Experimental details

The technique used for the nuclear states of interest (Fig.1) is *projectile Coulomb excitation* in combination with *TF* in ferromagnetic Gadolinium. The target, consisting of approximately 50 mg/cm^2 of ^{208}Pb and 50 mg/cm^2 of Gd, serves for excitation in Pb and Gd and spin precession in the Gd layer. The latter is observed via the rotation of the anisotropic angular correlation of γ rays emitted from the excited 2_1^+ and 4_1^+ states. Both precession and angular correlation are measured simultaneously with γ detectors at fixed polar angles

Θ_γ , in and close to the reaction plane, using a particle detector with azimuthal position sensitivity. In this geometry TF measurements were successfully carried out at beam energies of ~ 15 MeV/u [6]. At projectile energies of ~ 100 MeV/u, the strong Lorentz boost of the γ intensity distribution requires to set the γ detectors at forward angles, which is foreseen with the RISING detector array. (Fig. 2) The radioactive $^{132,134,136}Te$ and ^{138}Xe

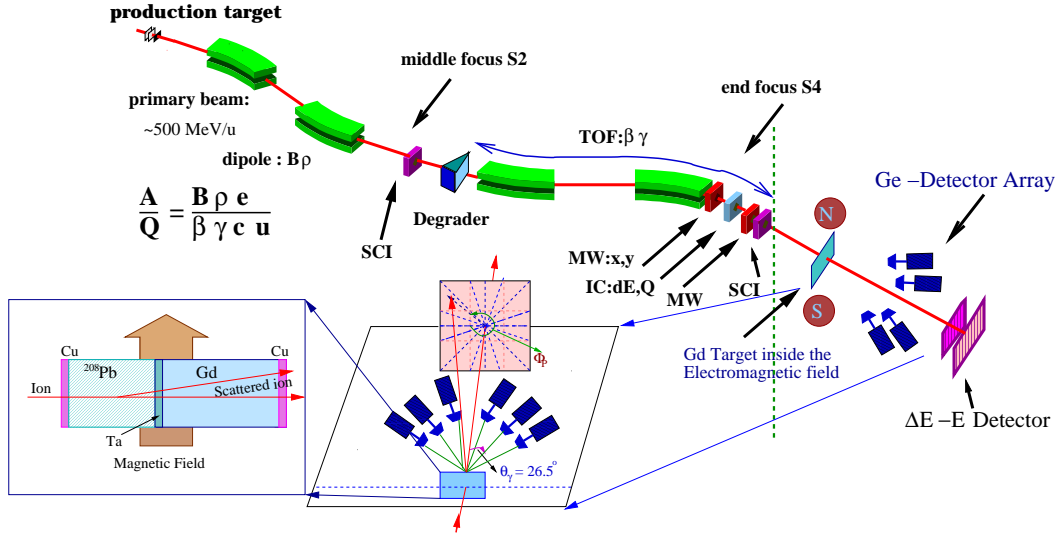


Figure 2: Schematic view of the fragment separator, various tracking detectors, the target assembly and the RISING detector array. Also displayed in more detail is the target composition.

projectiles will be produced in fragmentation reactions of stable ^{136}Xe and ^{164}Dy beams, respectively, accelerated by the SIS accelerator to energies of ~ 500 MeV/u. The secondary ions are separated with the fragment separator and will be focussed onto the double-layered target polarized by Gd external field of 0.08 Tesla. Ion tracking of the incoming and the scattered ions is required for Doppler-shift correction and well-defined determination of the interaction time of the ions in the ferromagnetic Gd layer. The de-excitation γ rays are measured with RISING Ge Clover detectors in coincidence with the scattered ions, registered in a position sensitive Si strip detector.

2.3 Angular correlation and precession

^{134}Te ions are produced in the fragmentation of a ^{136}Xe beam of 500 MeV/u on a 4 g/cm 2 Be target. The target for Coulomb excitation and precession of the excited states consists of 50 mg/cm 2 ^{208}Pb deposited on 50 mg/cm 2 thick Gd.

The separated ^{134}Te ions enter the entire target with an energy of ~ 100 MeV/u and exit at ~ 92 MeV/u. The mean energy in Gd corresponds to a velocity of $v_{ion} \simeq 60v_0$, which slightly exceeds the Bohr velocity, implying a H-like ion fraction of $q_{1s} \simeq 0.5$. From

COULEX calculations of the 2_1^+ state at 1279 keV one derives a mean transit time of the ions through the Gd layer $T = 0.5$ ps or $T = 0.23$, depending on the excitation in the Pb- or Gd-layer, respectively. The grazing angles in the center of mass frame are for Pb 2.9° and for Gd 2.7° .

For the TF strength in these conditions, using eqs. (1) and (2), with $p_{1s} = 0.03$, $q_{1s} = 0.5$ and $B_{1s}(Z = 52) = 3.05$ *MTesla*, and an estimated attenuation factor of the field, $G_{beam} \simeq 0.5$, due to the energy loss of the heavy ion beam in the target, one obtains:

$$B_{TF} \simeq 23 \text{ kTesla.}$$

With this effective TF one derives for effective interaction times, $t_{eff} \simeq 0.3$ ps and 0.2 ps for excitation in Pb or Gd, respectively, a total precession angle:

$$\frac{\Phi^{exp}}{g} = \frac{\mu_N}{\hbar} \int_{t_{in}}^{t_{out}} B_{TF}(v_{ion}(t)) e^{-\frac{t}{\tau}} dt \simeq 300 \text{ mrad,}$$

where t_{in} and t_{out} are the mean entrance and exit times of the ions in the Gd layer. For an estimated $g(2_1^+) = +0.8$ one obtains a precession angle:

$$\Phi^{exp}(2_1^+) \simeq 240 \text{ mrad.}$$

The expected angular correlation of the $(2_1^+ \rightarrow 0_1^+)$ γ rays of ^{134}Te in the rest frame of the emitting nuclei is shown in Fig.3. As the Te ions recoil out into vacuum, the anisotropy of the correlation will be attenuated by the strong hyperfine fields of $1s$ electrons in the dominant H-like ions, expressed by the attenuation coefficients G_2 and G_4 . In addition, a sensible calibration of the field can be accomplished in similar conditions with the known g factor of Coulomb excited $^{136}\text{Xe}(2_1^+)$ state.

3 Beam time request

In the following we give an estimate of the beamtime, requested for the determination of the angular correlation and precession aiming for a 10% accuracy of the 2_1^+ g factor of ^{134}Te , and a calibration of the TF with $^{136}\text{Xe}(2_1^+)$.

With an intensity of the primary ^{136}Xe beam of $\sim 10^{10}/s$ one can expect for the secondary beam of ^{134}Te ions an intensity of $\sim 10^6/s$. Due to the count rate limitations of the particle detection system, MUSIC, the maximum tolerable intensity of the Te ions on the target, however, is $\sim 2 \cdot 10^4/s$. With the Coulomb excitation cross-sections of 300 mbarn and 200 mbarn in Pb and Gd, respectively, one obtains in the γ photopeak a coincidence count rate of ~ 10 counts/h for both field directions 'up' and 'down'. This corresponds to a photopeak efficiency of $\sim 1\%$ compared to a total efficiency of $\sim 2.6\%$ of the whole RISING detector array. With essentially two γ detectors in the reaction plane and a 10% accuracy of the g factor one requires in each γ detector and field direction a total peak intensity of ~ 500 counts. This implies a total beam time of 7 days, composed of 5 days for the ^{134}Te measurements and 2 days for the calibration of the TF with $^{136}\text{Xe}(2_1^+)$. The latter requires ^{136}Xe as primary beam with an intensity of $\sim 10^6$ ions/s. This increased intensity can be tolerated as the limiting MUSIC detector is not needed.

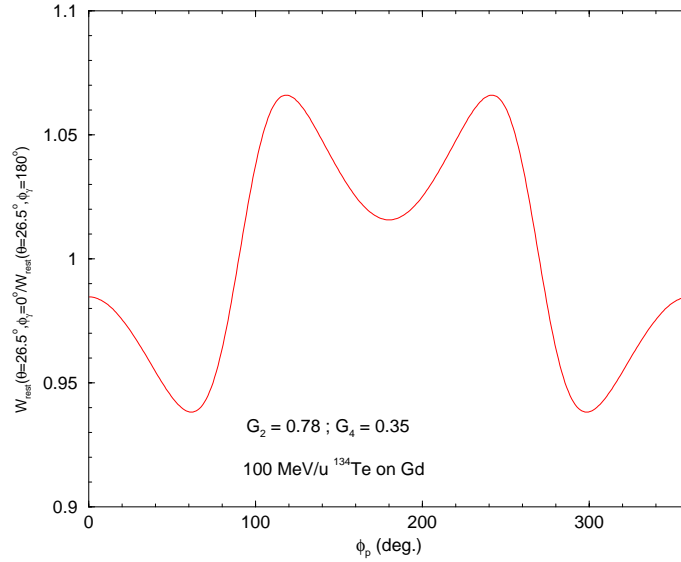


Figure 3: Particle- γ -angular correlation of Coulomb excited $^{134}\text{Te}(2_1^+)$ as ratio of γ intensities of two Ge detectors at angles $|\Theta| = 26.5^\circ$ symmetric to the beam direction, calculated as a function of the azimuth angle Φ_P of particle detection in the rest frame of the γ -emitting nuclei. G_2 and G_4 are the attenuation coefficients due to hyperfine interactions in vacuum [6].

References

- [1] J. Holden et al., Phys. Lett. **B 493** (2000) 7
- [2] O. Kenn et al., Phys. Rev. **C 63** (2000) 021302(R)
- [3] N. Benczer-Koller et al., Annu. Rev. Nucl. Part. Sci. **30** (1980) 53
- [4] G. J. Kumbartzki et al., Hyp. Int **7** (1979) 253
- [5] N. Rud and K. Dybdal, Phys. Scripta **34** (1986) 561
- [6] U. Grabow et al., Z. Phys. **A 359** (1997) 377
- [7] G. Jakob et al., Phys. Rev. **C 65** (2002) 024316
- [8] S. Wagner et al., Phys. Rev. **C 64** (2001) 034320

Search for stable octupole deformation in neutron-rich $^{142-144}\text{Ba}$ using relativistic Coulomb excitation

S. Mandal, F. Becker, J. Gerl, M. Górska, I. Kojouharov, Y. Kopatch,
H. Schaffner, H.-J. Wollersheim

Gesellschaft für Schwerionenforschung, Darmstadt, Germany

K.-H. Speidel

Institut für Strahlen- und Kernphysik, Univ. of Bonn, Germany

W. Urban

Institute of Experimental Physics, Warsaw University, Poland

1 Introduction

The atomic nucleus is a quantal many-body system and possesses a variety of shapes and sizes throughout the periodic table. The shape can be a sphere, an ellipsoid or a shape in between the two, depending on the number of protons and neutrons; some nuclei show the coexistence of different shapes. For nuclei at and near closed shells, the ground state is spherical and phase transition gradually occurs from spherical to deformed shapes as one moves away from closed shells. The observation of large quadrupole moments of rotational band structures and measurements of their properties have confirmed the deformed shape (spheroidal shape) of nuclei. For the majority of deformed nuclei a description assuming an axial and reflection symmetry (i e. symmetry under space inversion) is adequate to reproduce the band structure. In this case all the members of the rotational band will have the same parity. However, the observation of parity doublets in some nuclei suggests the possible existence of shapes, which are asymmetric under space inversion, the so called reflection-asymmetric shapes.

The calculations with a reflection-asymmetric mean-field (RAMF) predicted that the

reflection-asymmetric shapes (i.e., octupole deformation or octupole collectivity) appear in specific regions of the nuclear chart, where the Fermi level approaches pairs of close lying, opposite-parity orbitals with $\Delta j = \Delta l = 3$, which may be coupled by the octupole interaction. The strong octupole deformation or correlations are localized around particular proton and neutron numbers. The maximum octupole coupling occurs just above the closed shells viz. $Z, N = 34, 56, 88, 134$ where $(N|j)$ intruder orbitals interact with $(N-1, l-3, j-3)$ natural parity states through the octupole component of the mean field. Though about an order of magnitude weaker than the quadrupole one, the octupole residual interaction is of a fundamental importance because it correlates orbitals of opposite parity, leading to mixed-parity states in the reference frame of the nucleus. Such exotic states may, for instance, enhance the effect of "true" parity violation in weak interactions, thus making a nucleus a convenient laboratory to study this fundamental phenomenon. The increased binding of a nucleus, due to octupole interaction, which may be of the order of 1 MeV, may affect another important process, the astrophysical r process. It has been suggested recently, that enhanced octupole correlations are present in very neutron-rich Kr isotopes [1]. The presence of extra binding in these nuclei may influence the direction of the r -process path, running across this region. It is also worth mentioning that lower in magnitude but easy to discriminate from the dominating quadrupole residual interactions, the octupole component provides a more precise probing of the nuclear mean field. For all these reasons it is very important to localize on the nuclear chart and study in detail the effects of octupole residual interaction in nuclei. Detailed mean field calculations for the ground state predict that the strongest octupole deformation is present in the neutron deficient nuclei around ^{224}Th , with negative parity excitations of the order of 200 keV and in the neutron rich nuclei around ^{146}Ba , with the energy of the lowest 1^- state of about 750 keV [2].

In the present proposal we would like to investigate reflection asymmetric neutron-rich Ba isotopes in their ground and excited states. It has been a long standing question of whether octupole correlations in these nuclei are strong enough to produce stable octupole shapes at low excitation energy. Several theoretical calculations suggested the presence of a stable octupole deformation in $^{142-146}\text{Ba}$. It has been also speculated that the energy gain due to octupole deformation in Ba isotopes is insufficient to produce octupole-deformed shapes [3]. In the region of ^{146}Ba , octupole instability was first predicted by Nazarewicz et al. [4] using the Strutinsky-type potential energy calculations for axially symmetric

and reflection asymmetric deformations. Skalski [5] has also predicted the signature of octupole-deformed ground states in the above nuclei, where he calculated the deformation energy within the Strutinsky method with the Woods-Saxon mean field. The deformed shell model calculations yield large energy gaps at $Z=56$ and 62 in the proton spectrum due to octupole mixing between the $h_{11/2}$ and $d_{5/2}$ orbitals. For the neutron system there is a gap at $N=88$, which results from the octupole mixing between the $i_{13/2}$ and $f_{7/2}$ orbitals [6].

The observation of opposite-parity intertwined bands, connected by enhanced E1 transitions in ^{144}Ba [7], confirmed the theoretical prediction of octupole instability in this region. Later measurements by Mach et al [8] and Urban et al. [9] also confirmed this prediction. The experimental evidence for stable octupole-deformed shapes in $^{142-146}\text{Ba}$ is based on $B(E1)/B(E2)$ branching-ratios. Such simple estimates of β_3 based on $B(E1)/B(E2)$ branching-ratio values are not fully conclusive. More precise information can be obtained by performing direct measurements of electromagnetic transition probabilities. Such measurements could provide the conclusive information on stable octupole deformation in Ba isotopes. Using the Coulomb excitation technique the E3 matrix elements can easily be determined. In Coulomb excitation the probability for excitation of the 3^- state coupled by the E3 operator is much larger than that for E1 compared to de-excitation (the E1 transition rate is many orders of magnitude faster than that of E3).

Apart from verifying the existence of octupole deformation in Ba isotopes, the proposed experiment could help resolving another intriguing problem, concerning the octupole deformation in these nuclei. It has been noticed already by Phillips et al. [7], that the $B(E1)/B(E2)$ branching ratios in ^{146}Ba , indicated by the theory as the best place to look for the effect, are an order of magnitude smaller than in the neighboring ^{144}Ba isotope. This surprising observation prompted further calculations, which have explained low values of $B(E1)$ rates in ^{146}Ba as the result of a local cancellation the electric dipole moment D_0 in this nucleus. The D_0 , moment is a sum of the volume and the shell-correction contributions, which cancel each other in ^{146}Ba . This explanation was further supported by the observation of enhanced $B(E1)/B(E2)$ branching ratios in the next, ^{148}Ba isotope [9]. The discussed picture assumes that the volume contribution, originating from the octupole deformation of a nucleus, is non zero in ^{146}Ba . On the other hand the alignment process ob-

served in the ground-state band of ^{146}Ba , is characteristic of a reflection-symmetric shape. It is therefore of a great interest to verify the degree of octupole deformation in the ground state of ^{146}Ba via a direct measurement of the $B(E3)$ transition probability to the 3^- state.

Similar discrepancies are encountered in Ce isotopes. The theory predicts that octupole correlations in these nuclei are generally weaker than in Ba isotopes due to the $Z=56$ gap, and in the ^{148}Ce a reflection-symmetric shape is expected [6]. This disagrees with the recent observation of enhanced $B(E1)/B(E2)$ branching ratios in the discussed Ce isotopes [10]. Future, direct measurements of electromagnetic moments in these nuclei could further verify the presence of octupole deformation in the neutron-rich lanthanides.

In summary, we propose to investigate the neutron-rich even-even Ba ($A=140-146$) isotopes. We intend to measure the $B(E2)$, and $B(E3)$ values using presently available radioactive beams of those nuclei in order to study the stable octupole shapes. First we will investigate $^{142-144}\text{Ba}$ because of sufficient secondary beam intensity. The rates estimates for ^{146}Ba are rather pessimistic at the moment.

2 Experimental Method

We propose to use in-beam γ spectroscopy following relativistic Coulomb excitation to investigate the electromagnetic properties of these neutron-rich radioactive nuclei. For the present project, we intend to use 500-600 MeV/u ^{150}Nd beams from SIS to produce $^{142-144}\text{Ba}$. The fragments with energy of 100 MeV/u will be focused on the Pb target for Coulomb excitation of the first 2^+ and 3^- states. Standard FRS detection setup by combining measurements of the fragments' magnetic rigidity $B\rho$, their energy loss ΔE and their time of flight TOF, will be used for the tracking of the fragments before the COULEX target. The reaction products emerging downstream after interaction with the Pb target of 300 mg/cm² thickness will be identified by a E- ΔE telescope (CATE) which is a combination of position sensitive silicon PIN diode (to measure the position and ΔE) and CsI scintillator (for total energy E). The de-excitation γ -rays of the scattered beam particles will be detected by RISING Cluster detectors placed at forward angles.

3 Count Rate Estimates

We estimated the value of electromagnetic moments $B(E3)$ from the theoretically predicted β_3 [11] value for Ba isotopes. The total relativistic Coulomb excitation cross section has been calculated by using the Winther and Alder formalism [12]. In order to be free of nuclear excitation, the safe distance of closest approach used was 15.2 fm, which corresponds to scattering angles $\theta_{cm} \leq 3.0^\circ$ of the beam particles.

The experimentally observable $E(3^-)$ and $E(2^+)$ γ -ray transition rates, $N_\gamma(3^-)$ and $N_\gamma(2^+)$, have been estimated from the known secondary beam production rates. To estimate the secondary beam intensity and transmission through the FRS and size of beam spots at the secondary (COULEX) target position, a simulation has been performed using the ion-optics simulation code MOCADI [13]. The production cross section of secondary fragments was calculated by using EPAX2 [14]. We assumed a primary beam intensity of 5×10^9 particles per second. ^9Be of 4 g/cm^2 will be used as a primary production target. We use for Coulomb excitation a Pb target of 300 mg/cm^2 thickness. The secondary beam will be 100 MeV/u at the reaction target. The final count rates, $N_\gamma(3^-)$ after corrections for efficiency of the RISING Gamma detectors array are given in Table 1. The count rates $N_\gamma(2^+)$ of Ba isotopes are more than 10 times larger than $N_\gamma(3^-)$.

Table 1: Estimates of $B(E3)$, σ_{E3} and γ -ray transition count rates of $^{142,144,146}\text{Ba}$ nuclei

| Nucleus | Secondary Beam Intensity (PPS) | $E(3^-)$ (keV) | $B(E3)$ (e^2fm^6) | σ_{E3} (mb) | $N_\gamma(3^-)$ (per day) |
|-------------------|--------------------------------|----------------|-------------------------------------|--------------------|---------------------------|
| ^{142}Ba | 18300 | 1292.2 | 76501.3 | 7.03 | 240 |
| ^{144}Ba | 2099 | 838.0 | 98402.7 | 8.89 | 38 |
| ^{146}Ba | 104 | 821.3 | 100530.3 | 9.01 | 2 |

4 Beamtime Request

Based on the above count rate estimates (Table 1) we ask for the following beam time. For ^{144}Ba 15 shifts and for ^{142}Ba 9 shifts. This will allow a statistical precision in the measurement of the B(E3) values of 3 % to 10 %, depending on the particle count rates.

The total requested beam time : *24 shifts or 8 days*

References

- [1] T. Rząca-Urban et al., Eur. Phys. J. A 9, 165 (2000)
- [2] P.A. Butler and W. Nazarewicz, Rev. of Mod. Phys. **68** (1996) 349.
- [3] J.L. Egido and L.M. Robledo, Nucl. Phys. **A518** (1990) 475.
- [4] W. Nazarewicz et al., Nucl. Phys. **A429** (1984) 269.
- [5] J. Skalski, Phys. Lett. **B238** (1990) 6, Phys. Rev. **C43** (1991) 140.
- [6] W. Nazarewicz et al., Phys. Rev. **C45** (1992) 2226.
- [7] W.R. Phillips et al., Phys. Rev. Lett. **57** (1986) 3257.
- [8] H. Mach et al., Phys. Rev. **C41** (1990) R2469.
- [9] W. Urban et al., Nucl. Phys. **A613** (1997) 107.
- [10] E.Garrote, J.L.Egido and M.Robledo, Phys. Rev. Lett. 80, 4398 (1998)
- [11] A. Sobiczewski et al., Nucl. Phys. **A485** (1988) 16.
- [12] A. Winther and K. Alder, Nucl. Phys. **A319** (1979) 518.
- [13] Th. Schwab, GSI Report GSI-91-10 (1991).
- [14] K. Sümmerer and B. Blank, Phys. Rev. **C61** (2000) 034607.

Prompt gamma spectroscopy and isomer tagging. Deformation of five-quasiparticle states in the $A \approx 180$ mass region

Zs. Podolyák¹, P.M. Walker¹, J. Gerl² and the RISING collaboration

¹University of Surrey, UK; ²GSI, Darmstadt, Germany

GSI with the FRS has the unique capability of providing isomeric beams of heavy ions. The high resolution of RISING will allow the possibility to pick up low intensity γ -ray transitions from the continuum of the atomic background. This combination makes GSI an unique place for studying the physics of isomers, and encourages the development of new experimental techniques.

Shape is a basic property of the nucleus. It is relatively easy to determine it experimentally for the groundstate, but more difficult for excited states. In the case of multi-quasiparticle states, the determination of the deformation is needed for understanding the stability of axial symmetry and K-isomer decay rates [1]. However, this presents a real challenge due to technical difficulties. Few attempts have been made to measure the deformation of multi-quasiparticle isomers, and the results are sometimes controversial. In ¹⁷⁹W [2] the deformation of the $I=K=35/2$ five-quasiparticle isomer is less than that of the groundstate, contrary to the theoretical predictions. The situation is somewhat similar in ¹⁸²Os [3,2]. In contrast, in ¹⁷⁸Hf [4] and ¹⁷⁶W [5] similar groundstate and multi-quasiparticle state (high-K) deformations were measured (see fig. 1). The situation is unclear because of uncertainties coming from the techniques that have been used.

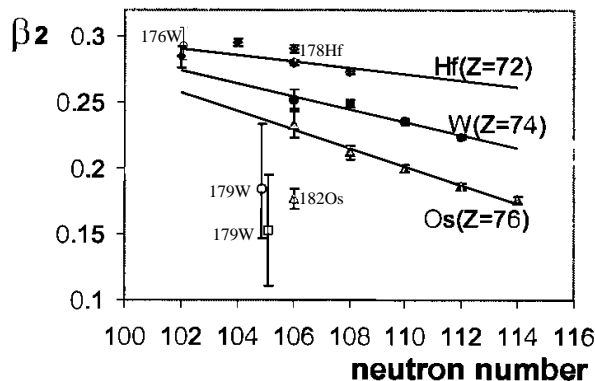


Figure 1: Quadrupole deformation of groundstate and multi-quasiparticle isomers in the $A \approx 180$ region (from [6]). The deformations of the multi-quasiparticle isomers are labelled.

Currently there are few methods to measure deformations (quadrupole moments). The quadrupole moment can be determined from its interaction with the lattice electric field gradient, in the case of isomers with lifetimes in the range 100 ns-1 ms. This technique gives results with large uncertainties originating from insufficient knowledge of the electric field gradient and its temperature dependence in crystals. In the case of longer lived isomers, the quadrupole moment can be determined by studying the atomic hyperfine spectrum with lasers, but few such isomers are accessible.

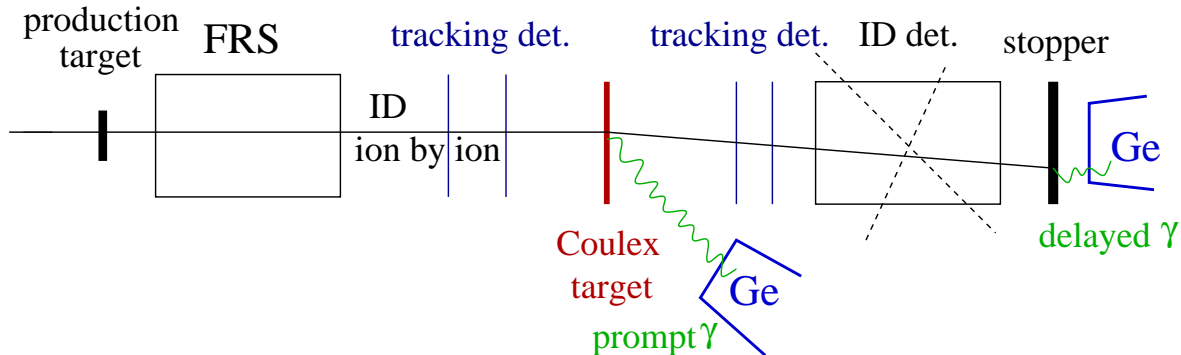


Figure 2: Experimental setup for the Coulomb excitation experiments at the FRS. The setup can be used to study Coulomb excitation of both the groundstates and isomeric states. However, the identification detectors after the secondary target are not needed when the Coulex of isomers is investigated.

Here we propose to measure the quadrupole moments of multi-quasiparticle states by Coulomb exciting them. Since the mechanism of Coulomb excitation is well known, the obtainable values will be accurate (depending only on statistics). The use of fragmentation reactions at the FRS will allow the employment of this method also in the case of neutron-rich nuclei.

Previous experiments have shown that isomeric beams can be produced in projectile fragmentation, with intensities up to 20% of the total intensity of a given nuclide [7]. The ions in an isomeric state can be Coulomb excited on a lead target at the final focal point of the FRS. The proposed experimental setup is shown in fig. 2. The prompt gamma-rays will be detected with RISING. Further on, the beam will be stopped in a catcher and the decay out of the isomer will be detected with some additional γ -ray detectors (Ge or NaI). This isomeric decay will be used as a tag, to give us the identification of the ion after the Coulomb excitation target (before the target the identification is made with the FRS). In order to have an unambiguous correlation between the delayed γ rays and the incoming ions, the isomers should have lifetimes less than 100 μ s.

Technically, the Coulomb excitation of isomeric states is simpler than the more traditional Coulex of groundstates (at the FRS). In the latter case, the ions have to be identified after the Coulex target using magnetic fields, ion chambers, total energy detectors etc., a very difficult task in the case of heavy ions. In the case of the Coulomb excitation of isomeric states, the γ -rays deexciting the isomers can be used as a tag to identify the ions after the Coulex target. The feasibility of these experiments depends mainly on the background in the prompt spectra (at the Coulex target), where the atomic background might obscure the Coulex γ -rays. (This problem is common for all the Coulex experiments).

The Coulex of the isomer gives not only the transition probabilities, but the energies of the states based on the isomer. This is important in the case of neutron-rich nuclei, where these states cannot be identified using other methods.

We propose to use the presented technique to study the deformation of 5-quasiparticle

isomers in the $A \approx 180$ region. Such structures were populated in ^{175}Hf , ^{179}W and ^{181}Re during our previous projectile fragmentation experiment [7]. These five-quasiparticle states with spin $I=K=35/2$ represent the highest discrete spin observed so far in fragmentation reactions. Because of their multi-quasiparticle character, they present an ideal case to test the change in deformation compared to the groundstate. In addition, the transition between the well deformed nucleus ^{175}Hf to the relatively gamma-soft ^{181}Re can be studied at high spins.

The halfives of these isomers, between 0.75 and 1.2 μs , are ideal for the presented technique. They live long enough to survive the flighttime of a few hundred nanoseconds between the production target and the stopper, and decay fast enough to minimise random coincidences. The rotational structures based on the isomers are shown in fig. 3.

The experiment can be performed using either ^{208}Pb or ^{238}U as the primary beam. The expected rates are calculated for the $I=35/2$ isomer in ^{179}W using a ^{208}Pb beam. The number of ^{179}W ions produced in fragmentation is: $\sigma \times I_{\text{beam}} \times N_{\text{target}} = 0.952 \text{ mb}$ (measured [11]) $\times 10^8/\text{s} \times 10^{23} \text{ nuclei/cm}^2$ (1.6 g/cm^3 Be target) $= 10^4$ ^{179}W ions/s. 2.7% of the ions [7], that is 270 s^{-1} , will be produced in the $I=35/2$ isomeric state. The Coulomb excitation cross section on a ^{208}Pb target is estimated [12] to be 123 mbarn and 2327 mbarn for the $35/2 \rightarrow 39/2$ and $35/2 \rightarrow 37/2$ excitations, respectively (these are lower than that of the groundstate because the effect of the Clebsch-Gordan coefficients). Using a 300 mg/cm^2 ^{208}Pb (10^{21} atoms/ cm^2) target and assuming a 5% gamma-ray detection efficiency, 5.98 hour^{-1} 379 keV $39/2 \rightarrow 37/2$ and $5.98 \times (18.92 + 1) = 119 \text{ hour}^{-1}$ 363 keV $37/2 \rightarrow 35/2$ γ -rays will be detected. (Here we omitted the M1 Coulomb excitation, which would further increase the intensity of the 363 keV line.) If we require a coincidence between the delayed γ -ray from the isomer and the prompt Coulomb excitation γ -ray, we reduce the rate of the 363 keV transition to 12 hour^{-1} , assuming 10% detection efficiency for the delayed γ rays, but the atomic background is reduced by a factor of 370. In two days we can collect 576 counts, which gives us the deformation with an accuracy of $\approx 2\%$ (no radiation background is considered), which is a factor 10 better than the previous value [2]. However, the finally achieved accuracy will depend on the level of the background (atomic+nuclear) radiation, and we expect more realistically to achieve a $\approx 4\%$ accuracy in 2 days. At a secondary beam energy of 100 MeV/nucleon, corresponding to a velocity of $\beta=0.43$, the Doppler shift of the 363 keV $37/2 \rightarrow 35/2$ transition at $\theta=30^\circ$ is 160 keV, and it will be detected at 522 keV in the RISING detectors. This energy is much higher than the maximum energy of the atomic background, which is 230 keV for 100 MeV/nucleon, and it is not Doppler shifted. (The maximum secondary beam energy for which the background limit is below the line of interest is 244 MeV/nucleon.)

Similar rates are expected for the other two $I=K=35/2$ isomers. By using ^{238}U beam, the isomeric ratio is probably higher.

6 days of beamtime (1 GeV/nucleon ^{208}Pb or ^{238}U) is requested in order to measure with high accuracy the deformation of the $I=K=35/2$ isomers in ^{175}Hf , ^{179}W and ^{181}Re , i.e. two days for each isomer.

We note that the same FRS setup will allow us to study other lower spin isomers, and therefore to follow the change in deformation as quasiparticle pairs are broken. Generally, these states are characterised by higher isomeric ratios and higher transition strenghts

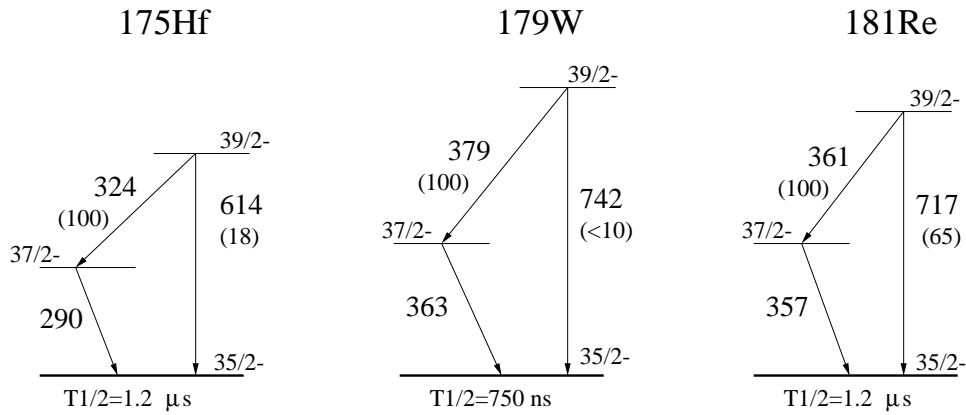


Figure 3: Rotational structures built on the $I=K=35/2$ five-quasi-particle isomers in ^{175}Hf [8], ^{179}W [9] and ^{181}Re [10]. The branching ratios are given in brackets.

(mainly due to the Clebsch-Gordan coefficients). Consequently, they will give better statistics. However, the lower Coulex transition energies will lead to a larger background in the spectra. The determination of the relative quality of the data is an important element of this primary experiment. An example of such a lower-spin isomer is: ^{179}W , $I^\pi=21/2^+$, $I_R=6(1)\%$, $T_{1/2}=0.39\mu\text{s}$; and it may be possible to measure simultaneously in adjacent nuclei other isomers.

- [1] P.M. Walker, G.D. Dracoulis, Nature 399 (1999) 35.
- [2] D. Balabanski et al., Phys. Rev. Lett. 86 (2001) 604.
- [3] C. Broude et al., Phys. Lett. B264 (1991) 17.
- [4] N. Boos et al., Phys. Rev. Lett. 72 (1994) 2629.
- [5] M. Ionescu-Bujor, private communication.
- [6] G. Neyens et al., Acta Phys. Pol. B32 (2001) 1061.
- [7] M. Pfützner et al., Phys. Rev. C., in press.; M. Pfützner et al., Acta Phys. Pol. B32 (2001) 2507.
- [8] F. Kondev, private communication.
- [9] P.M. Walker et al., Nucl. Phys. A 568 (1994) 397.
- [10] C.J. Pearson et al., Nucl. Phys. A 674 (2000) 301.
- [11] M.de Jong et al., Nucl. Phys. A628 (1998) 479.
- [12] A. Winther, K. Alder, Nucl. Phys. A319 (1979) 518.

Investigation of the structure and deformation of $^{185-187}\text{Pb}$ by γ -spectroscopy and lifetime measurements

J. Gerl, et al., *Darmstadt*

A. Andreyev et al., *Liverpool*

G.D. Dracoulis et al., *Canberra*

W. Meczynski, J. Styczen et al., *Krakow*

MOTIVATION

The light Pb isotopes are a particularly interesting testing ground for the nuclear shell model. Due to the $Z=82$ magic gap they are spherical in their ground states. Proton pair excitation across the $Z=82$ shell coupled to spin and parity 0^+ comes low in energy. This is due to the creation of one particle and one hole pair which yields a gain in pairing correlation energy. Furthermore, the attractive proton-neutron interaction lowers the energy of the 2p-2h states, so that for even Pb isotopes with mass $A \leq 194$ the corresponding 0^+ state lies below the first excited 2^+ state. Within a deformed mean-field approach this is equivalent to a macroscopic phase change from a spherical to an oblate shape. The band structure built on top of it has been observed only for a limited number of isotopes, the lightest being ^{190}Pb .

This schematic picture can also be extended to multi-particle and multi-hole excitations, each of them possibly leading to a different shape. The large space available for valence neutrons (mid-shell between $N=82$ and $N=126$) favours deformed configurations. Combined with the strength of the proton-neutron quadrupole force and the pairing, a subtle balance originates where the promotion of specific proton pairs to the next shell leads to either a prolate or to an oblate state. At lighter masses (Sn and Ni region), the steady increase in the shell gap energy, combined with a decreasing open space for the valence particles, lead to an increase in excitation energy of deformed states. For heavier elements the shell gap becomes too narrow and the proton-neutron correlation causes the ground state to become deformed. Therefore, only the n-deficient Pb region shows dramatic shape changes close to the ground state where the level density is low. Thus, it provides ideal conditions to study the microscopic origin of the spherical-symmetry breaking which leads to spheroidal deformation.

A 4p-4h state has been associated to a recently discovered 0^+ state in ^{186}Pb [1] establishing the only triple shape coexistence of low-lying 0^+ states found so far. Based on the energy systematics of the oblate band heads in the heavier Pb isotopes, the extrapolation of the 0^+ band-head energy starting from the higher-spin members of a band assumed to be prolate deformed [2,3] and reduced α -decay widths, the first excited 0^+ state at 532 keV has been assigned oblate and the second excited 0^+ state at 650 keV prolate deformed.

This characterization is supported by detailed potential-energy-surface calculations (see fig. 1) predicting quadrupole deformations around $\beta_2 \approx 0.15$ and $\beta_2 \approx 0.27$ for the oblate respectively prolate shape as well as super and hyper-deformed states at higher excitation energy [4,5]. To proof this scenario true, experimental determination of deformation parameters for ^{186}Pb is helpful. Moreover, the level scheme of the low lying non-yrast states needs to be determined to perform mixing calculations. This new structure information will help to pin down the parameters used in the calculations, leading to an improved understanding of subtle shell effects and a better predictability of exotic shapes.

Triple shape coexistence is predicted for the odd neighbours $^{185,187}\text{Pb}$ too. Low lying states are known from α -decay measurements, e.g. at 226 keV and 280 keV in ^{185}Pb [6] interpreted as prolate deformed. Again, deformation parameters and any additional information on the decay scheme is very valuable.

We propose to measure the lifetime of the 4^+ state at 923 keV in ^{186}Pb assumed to be prolate deformed, the states at 226 keV and 280 keV in ^{185}Pb and possibly of other low lying states in $^{185-187}\text{Pb}$, in order to deduce corresponding deformation parameters. In addition, detailed γ -spectroscopy is planned to clarify the low lying level structure in these nuclei. As a by-product, isomers (hampering fusion-evaporation type experiments) can be identified and transitions above isomers selected.

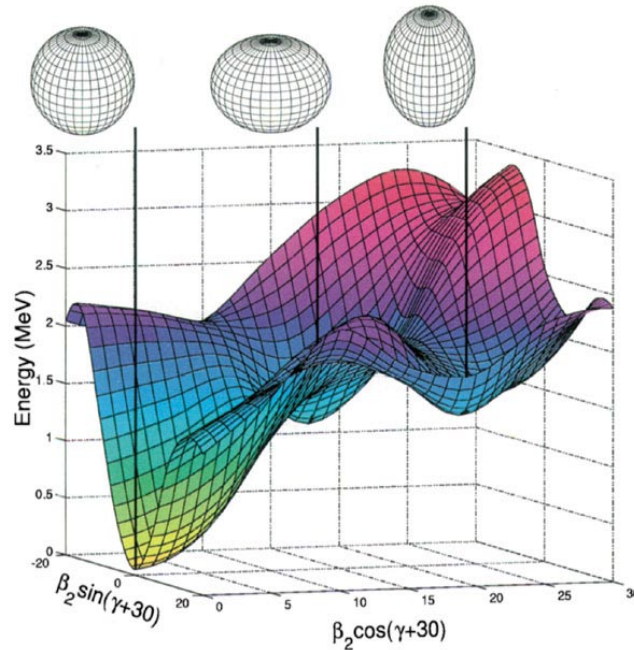


Fig. 1 Calculated potential energy surface for ^{184}Pb showing spherical, oblate and prolate minima at rather low energies (from [1]).

Experimental details

We propose to use a secondary fragmentation reaction to populate excited states in $^{185-187}\text{Pb}$ and to measure the lifetime of the states of interest by their γ -decay employing a differential Doppler shift method with a stack target. For that purpose ^{200}Rn produced by fragmentation of a 600 MeV/u ^{238}U beam on a ^9Be target is selected by the FRS and identified by the standard Rising set-up. The following rate estimation follows the assumptions made in the general Rising proposal. Although the nuclei of interest could be produced directly by ^{238}U fragmentation their cross section (e.g. $\sigma(^{186}\text{Pb}) = 260 \mu\text{b}$) is too small -compared to the total fragmentation and fission cross section- to be separable from the overwhelming contribution from other channels. Moreover, the rate capability of the particle tracking system would severely limit the usable primary beam intensity and thus turn the yield of $^{185-187}\text{Pb}$ down. In the proposed two-step process ^{200}Rn is produced with $\sigma(^{200}\text{Rn}) = 2.1 \text{ mb}$. Assuming a primary ^{238}U intensity of $6 \cdot 10^7 / \text{s}$ about $10^4 / \text{s}$ ^{200}Rn projectiles are available behind the FRS embedded in $\approx 4 \cdot 10^4 / \text{s}$ other beam species which are indeed distinguishable by the tracking detectors.

Using a secondary Al target consisting of three foils with 1.5 mm and 5 mm spacing respectively, and a total thickness of 0.5 g/cm^2 , the yield of ^{186}Pb produced with $\sigma(^{186}\text{Pb}) = 2.9 \text{ mb}$ is about $0.5 / \text{s}$. The corresponding yields for ^{185}Pb and ^{187}Pb is about $0.2 / \text{s}$ respectively $1 / \text{s}$. About 10% of the total fragmentation and fission yield go into these three channels of interest. Therefore the selectivity of the CATE system is adequate to reduce unwanted channels and fission events. A single isotope selection is not required since the resolution of the γ -detectors enables to distinguish lines from neighbour nuclei (gating on unknown lines on the other hand allows for an unambiguous determination of the mass and charge of the corresponding nucleus).

It can be assumed that the decay of most of the highly excited Pb fragments will proceed through yrast or close to yrast states. According to recent investigation [7] the most strongly populated spin is around $6 \hbar$ and the spin distribution should reach values up to $20 \hbar$. Taking into account the efficiency of the Ge detectors and internal conversion a final full energy γ -rate of about $30 / \text{hour}$ for the $260.6 \text{ keV } 4^+ \rightarrow 2^+$ transition in ^{186}Pb and about $5 / \text{hour}$ for the transition of the 280 keV state to the ground state of ^{185}Pb is estimated if a population probability of 50% and 20% is assumed. Following the above discussion the lifetime of the two transitions could be 30 ps and 20 ps leading to characteristic line shapes with the stack target, which is sensitive to lifetimes between about 0.2 ps and 50 ps . It should be mentioned that the background from atomic Bremsstrahlung does not exclude the measurement of 260 keV γ lines (or even lower energies) since selecting the 14 nucleon removal channel in itself biases nuclear de-excitation (The “prompt flash” problem only arises if the purely atomic interaction events can not be distinguished from nuclear interaction events, e.g. Coulomb excitation without trajectory selection).

To be able to identify isomers by their delayed γ -decay it is suggested to surround the E-detector of CATE by a compact array of fast BaF detectors. The useful time range is

from 50ns to 5 μ s, limited by the prompt radiation and the background from uncorrelated projectiles.

To reach sufficient statistical accuracy for the determination of the lifetimes about 10^3 full energy γ -events are required. Therefore about 1.5 days would be sufficient for ^{186}Pb , whereas 8 days are required for ^{185}Pb . These 8 days are very useful for the spectroscopy of ^{186}Pb , since they will enable measurement of $\gamma\gamma$ -coincidences for cascade decays. Thus a total **beam time of 8 days** is asked for.

References

- [1] A.N. Andreyev et al., Nature 405, 430 (2000)
- [2] J. Heese et al. Phys. Lett. B302, 390 (1993).
- [3] A.M. Baxter et al. Phys. Rev C48, R2140 (1993).
- [4] W. Nazarewicz Phys. Lett. B305, 195 (1993).
- [5] N. Tajima et al., Nucl. Phys. A551, 409 (1993).
- [6] A.N. Andreyev et al., Eur. Phys. J. A6, 381 (1999).
- [7] M. Pfuetzner et al., Phys. Rev. C accepted for publication .

Appendix B

List of institutions collaborating in RISING

HMI Berlin, Germany
Univ. Bonn, Germany
GANIL, Caen, France
Univ. Camerino, Italy
NBI Copenhagen, Denmark
IFJ Cracow, Poland
Univ. Cracow, Poland
CLRC Daresbury, UK
GSI Darmstadt, Germany
TU Darmstadt, Germany
Univ. Demokritos, Greece
Univ. Firenze, Italy
INFN Genova, Italy
MPI Heidelberg, Germany
FZ Jülich, Germany
Univ. Keele, UK
Univ. Köln, Germany
INFN Legnaro, Italy
Univ. Leuven, Belgium
Univ. Liverpool, UK
Univ. Lund, Sweden
Univ. Manchester, UK
Univ. Milano, Italy
LMU. München, Germany
TU. München, Germany
INFN/Univ. Napoli, Italy
CSNSM Orsay, France
IPN Orsay, France
INFN/Univ. Padova, Italy
Univ. Paisley, UK
FZ Rossendorf, Germany
CEA Saclay, France
Univ. Stockholm, Sweden
Univ. Surrey, UK
IPJ Swierk, Poland
Univ. Warsaw, Poland
Univ. Uppsala, Sweden
Univ. York, UK

